NASA Conference Publication 10074

Sand and Dust on Mars

Workshop Sponsored by the NASA Mars Science Working Group at the Department of Geology Arizona State University, Tempe, Arizona February 4-5, 1991

NASA

NASA Conference Publication 10074

Sand and Dust on Mars

Edited by
Ronald Greeley
Arizona State University
Tempe, Arizona

Robert M. Haberle
Ames Research Center
Moffett Field, California

Workshop Sponsored by the NASA Mars Science Working Group at the Department of Geology
Arizona State University
Tempe, Arizona
February 4-5, 1991

National Aeronautics and Space Administration

Scientific and Technical Information Branch

1991

TABLE OF CONTENTS

INTRODUCTION, SAND AND DUST ON MARS

Ronald Greeley
Department of Geology, Arizona State University
Tempe, AZ 85287-1404

Sand and Dust. There is a difference between these two sets of particles, and anyone concerned with windblown material on Mars or any other planet must be familiar with the distinctions. Sand refers to particles between about 60 and 2000 μm in diameter; dust refers to particles smaller than about 20 μm in diameter; both are independent of composition. What happens to particles 20 to 60 μm in diameter? On Earth there is a general lack of grains of this size, which is thought to be due to a combination of the rocks and processes that contribute to the production of small particles in general. We do not know if the same is true of the evolution of particles on Mars.

Aside from the size distinction between sand and dust, there are fundamental differences in the behavior of the two classes of particles. First is the minimum windspeed needed to move particles of specific sizes. Termed the *threshold "friction" velocity*, this parameter is related to the surface shear stress imparted by the atmospheric boundary layer to the ground. Extensive wind tunnel experiments and field measurements show that as sand size decreases, lower winds are required for threshold, until the size of about 80 μm in diameters is reached. This is the size that is most easily moved by the gentlest wind. The threshold curve then *increases*, with decreasing particle size, so that finer and finer dust becomes progressively more difficult to entrain by the wind. The reasons for this relationship are related to aerodynamic effects (small grains like dust are immersed in a laminar sublayer below the turbulent boundary layer) and to the greater influence of interparticle forces (such as electrostatic forces) on smaller grains.

Once particles are set into motion (i.e., "threshold" is achieved) there is a fundamental difference in the mode of transportation by the wind for sand and for dust. Most dust particles--once set into motion--are carried aloft in *suspension* and maybe carried long distance before they settle to the ground. In contrast, most sand grains move in a series of short "hops", called *saltation*, in which the grain bounces along the surface in trajectories which seldom exceed a meter or so in height. As saltating grains return to the surface they achieve their greatest speed, having been accelerated by the wind, and "splash" into other grains, setting them into motion by pushing them along the surface, ejecting them into suspension, or by initiating saltation in a cascading effect.

Experiments under martian conditions show that the general distinctions between sand and dust on Earth also apply to Mars. Thus, even though the wind speeds needed to initiate particle motion are much higher on Mars than on Earth because of the lower martian atmospheric density, the general shape of the threshold curve is the same, and the size grain most easily moved remains the same at about 100 μm in diameter.

Even before planetary exploration via spacecraft, there was speculation about duststorms on Mars. Earthbased telescopic observations showed color and albedo patterns that appeared, disappeared, and shifted with Mars seasons, and these changes were attributed by some planetologists to the growth and decay of duststorms.

Mariner 9, and later Viking, showed abundant evidence for aeolian, or windblown processes, and landforms on Mars. In the nearly two decades of analysis of spacecraft data, laboratory experiments, and development of various numerical models, a great deal has been learned about sand and dust on Mars. However, there is also much that remains unknown. Yet,

from both an engineering and scientific prospective, windblown sand and dust play an important role in planning for future missions. Infiltration of dust into spacecraft components, abrasion by windblown sand, roving vehicles becoming stuck in loose sand and dust, the influence of windblown material in the collection of scientific samples for analysis, and the interpretation of remote sensing observations are but some of the considerations that must be taken into account for future missions to Mars.

This workshop is designed to provide a forum for spacecraft engineers/mission designers and representatives from the scientific community knowledgeable of windblown sand and dust on Mars to discuss common interests. The goals were to determine which parameters are important for future missions, both from an operational point of view, and a scientific perspective, and to assess what is currently known, inferred, or "guessed" about these parameters. Results are shown in Table 2.

The workshop concluded with a discussion of studies that need to be undertaken to shed further light on problems related to sand and dust on Mars, as indicated in Table 3.

Acknowledgements

The workshop was sponsored through the Mars Science Working Group, chaired by Michael H. Carr, and supported by the Offices of Advanced Planning and Planetary Geosciences, Solar System Exploration Division of NASA.

Table 1. Participants in workshop on sand and dust.

Dr. Amos Banin
NASA-Ames Research Center
Mail Stop 239-12
Moffett Field, CA 94035-1000
(415) 604-6631

Dr. Al Binder
Lockheed Engineering and Sciences Corp.
Houston, TX 77058
(713) 538-1332

Mr. Dan Blumberg
Department of Geology
Arizona State University
Tempe, AZ 85287-1404
(602) 965-7037

Dr. Roger Bourke
Jet Propulsion Laboratory
Mail Stop 180-402
4800 Oak Grove Drive
Pasadena, CA 91109
(818) 354-5602

Dr. Philip Christensen
Department of Geology
Arizona State University
Tempe, AZ 85287-1404
(602) 965-7105

Dr. Todd Clancy
LASP-Campus Box 392
University of Colorado
5525 Central
Boulder, CO 80309-0392
(303) 492-6998

Dr. James Gaier
NASA-Lewis Research Center
Mail Stop 302-1
Cleveland, OH 44135-3191
(216) 433-2311

Dr. Matthew Golombek
Jet Propulsion Laboratory
Mail Stop 183-501
4800 Oak Grove Drive
Pasadena, CA 91109
(818) 354-3883

Dr. Ronald Greeley
Department of Geology
Arizona State University
Tempe, AZ 85287-1404
(602) 965-7045

Dr. Robert Haberle
NASA-Ames Research Center
Mail Stop 245-3
Moffett Field, CA 94035-1000
(415) 604-5491

Dr. G. Barry Hillard
NASA-Lewis Research Center
Mail Stop 202-1
Cleveland, OH 44135
(216) 433-2220

Dr. Scott Hubbard
NASA-Ames Research Center
Mail Stop 244-10
Moffett Field, CA 94035-1000
(415) 604-5697

Dr. James Iversen
Department of Aerospace Engineering
Iowa State University
Ames, IA 50010
(515) 294-5157

Dr. Bruce Jakosky
LASP - Campus Box 392
University of Colorado
Boulder, CO 80309-0392
(303) 492-8004

Mr. David L. Kaplan
Mail Code XE
Lunar and Mars Exploration Program Office
Lyndon B. Johnson Space Center
Houston, TX 77058
(713) 283-5416

Dr. Joe Kolecki
NASA-Lewis Research Center
Mail Stop 302-1
Cleveland, OH 44135
(216) 433-2296

Dr. Rodman Leach
NASA-Ames Research Center
Mail Stop 242-6
Moffett Field, CA 94035-1000
(415) 604-6427

Dr. Steven Lee
LASP, Campus Box 392
University of Colorado
Boulder, CO 80309-0392
(303) 492-5348

Dr. Michael Malin
Department of Geology
Arizona State University
Tempe, AZ 85287-1404
(602) 965-4335

Dr. Henry Moore
U.S. Geological Survey
Branch of Astrogeologic Studies
Mail Stop 946
345 Middlefield Road
Menlo Park, CA 94025
(415) 329-5175

Dr. Gary Olhoeft
U.S. Geological Survey
P.O. Box 25046
Mail Stop 964
Denver Federal Center
Denver, CO 80225
(303) 236-1302

Dr. David Paige
Department of Earth and Space Sciences
University of California, Los Angeles
Los Angeles, CA 90024
(213) 825-4268

Dr. Jeffrey Plescia
Jet Propulsion Laboratory
Mail Stop 183-501
4800 Oak Grove Drive
Pasadena, CA 91109
(818) 354-6936

Dr. Davis Sentman
TRW Systems Group RI/1170
One Space Park
Redondo Beach, CA 90278
(213) 812-0072

Dr. Charles H. Simonds
Lockheed Life Support Dev. Lab
Mail Code A-23
1150 Gemini Drive
Houston, TX 77058-2742
(713) 282-6203

Mr. Mark Sluka
Lockheed Engineering and Sciences Corp.
Houston, TX
(713) 283-5769

Dr. Paul Wercinski
NASA-Ames Research Center
Mail Stop 244-10
Moffett Field, CA 94035-1000
(415) 604-3157

Dr. Bruce White
Department of Mechanical Engineering
University of California at Davis
Davis, CA 95616
(916) 752-6451

Dr. Richard Zurek
Jet Propulsion Laboratory
Mail Stop 169-237
4800 Oak Grove Drive
Pasadena, CA 91109
(818) 354-3725

Table 2. Values for key parameters dealing with Sand and Dust on Mars (February, 1991)

	Parameter	*Measurement*	*Model*	*Ideas*	*Notes*
Particles in the Atmosphere (Haberle and Zurek)	Composition		> 60% SiO_2 1% magnetite		SiO_2 measurements based on inferences from Mariner 9 IRIS spectra - loosely constrained. Value quoted is higher than Viking lander soil elemental composition measurements.
	Density			ρ = 2 to 3 gm/cm^3	Based on typical silicate rock densities. Considered a good estimate.
	Size distribution		*range:* r = 0.1 to 10 μm *mean:* r = 0.4 to 2.5 μm		Measurements based on inferences from Mariner 9 IRIS spectra and Viking Lander Sun Diode images. Considerable uncertainty in concentrations of sub-micron particles. Means are cross-sectional weighted.
	Concentration		$N \sim N_0 \tau \exp(-z/H)$ where N_0 = 6 particles/cm^3, τ is the visible optical depth, z is height (km), and H = 10 km is an atmospheric scale height.		Based on the Mariner 9 inferred particle size distribution assuming r = 2.5 μm and ρ = 3 gm/cm^3
	Vertical distribution	Background dust haze extends 20 to 40 km above the surface. During dust storms, particles can reach 40 to 60 km		*Background dust haze:* particles are uniformly distributed with height. *Developing storms:* particles are concentrated near the surface in source regions; aloft elsewhere. Particles with radii >> 5 μm fall out quickly.	Consistent with twilight observations and sky brightness measurements. Loosely constrained.
	Geographical distribution	*Dust storm periods:* regional to global. *Non-dust storm periods:* localized storms can occur anywhere.		Maximum, concentrations tend to occur in tropical regions.	Highly variable.
	Seasonal distribution	Maximum dust loading occurs during southern spring and summer.			

Particles, in Atmosphere (Haberle and Zurek)	Optical properties	Solar optical depth varies from 0 to 6 or above.	τ_{vis}/τ_{ir} ~2 solar transmissivity ~ $\left(1+\frac{\tau}{2\mu}\right)^{-1}$		Optical depth always > 0.2 at the Viking lander sites. Solar transmissivity is that for purely scattering dust particles, and is therefore an approximation.
	Ground visibility		Visual range (km) ~ 10 / τ		Visual range for distinguishing a black target against a diffuse white background.
	Space-to-ground visibility	No surface features were visible from orbit during the first half of the 1971 storm.			
Physical Properties (VL-Sites) (Moore)	Particle size		0.1 to 2000 μm		"dust" to sand size
	Particle hardness		1 to 7, Moh's hardness scale		clay to silicate grains
	Particle shape		tabular, angular, rounded		
	Clod size		0.1 to 4 cm		
	Clod hardness		< 2, Moh's hardness scale		
	Particle density		2.6 to 3.0 g/cm^3		clay to basalt sand
	Bulk density		.87 to 2.0 g/cm^3		"dust" to sand
	Friction angle		18° to 40°		near-surface; loose "dust" to sand
	Cohesion		0 to 20 kPa		near-surface; loose sand to cemented soil
	Adhesion		0.9 to 79 Pa		
	Angle of response				Needs work by soil-engineer
	Bearing strength				Needs work by soil-engineer
	Penetration resistence				Needs work by soil-engineer

Electrical Properties (Olhoeft)	Conductivity				Soil should be excellent insulator
	Dielectric characteristics		$K' = 1.9^d$		d = bulk density in gm/cm^3
	Electrostatic effects			may be significant	
	Magnetic effects	1 to 10% Fe-bearing minerals			not a problem(?)
	Effects on Telecommunication				not a problem
Particle Composition (Banin)	Elemental	Available from XR-F, GCMS (see tables)			Measured at two Viking lander sites
	Mineralogy		Clay minerals Montmorillanite Nontronite Zeolites Pyrrhotite Maghemite Sulfates Salt NaCl	Scapolite Palagonites	Modelled for Viking lander sites
	Reactivity	GeX, LR experiments	Many models; 6.5 tons soil → 1 mole O_2		
	Toxicity				Not known
Wind Erosion (Greeley)	Abrasion rate		0 to 2 x 10^{-2} cm/yr		Dependent upon particle supply and material
	Particle speed		0 to 40% of windspeed		
	Flux		0.4 to 2.0 gm/cm•sec		
	Flux with altitude				Not known
Particles on Surface, Global (Christensen)	Size distribution		Based on Viking IRTM, and photogeology, see maps		See maps that follow

ROCK ABUNDANCE ON MARS, WESTERN HEMISPHERE

(from Christensen, 1986)

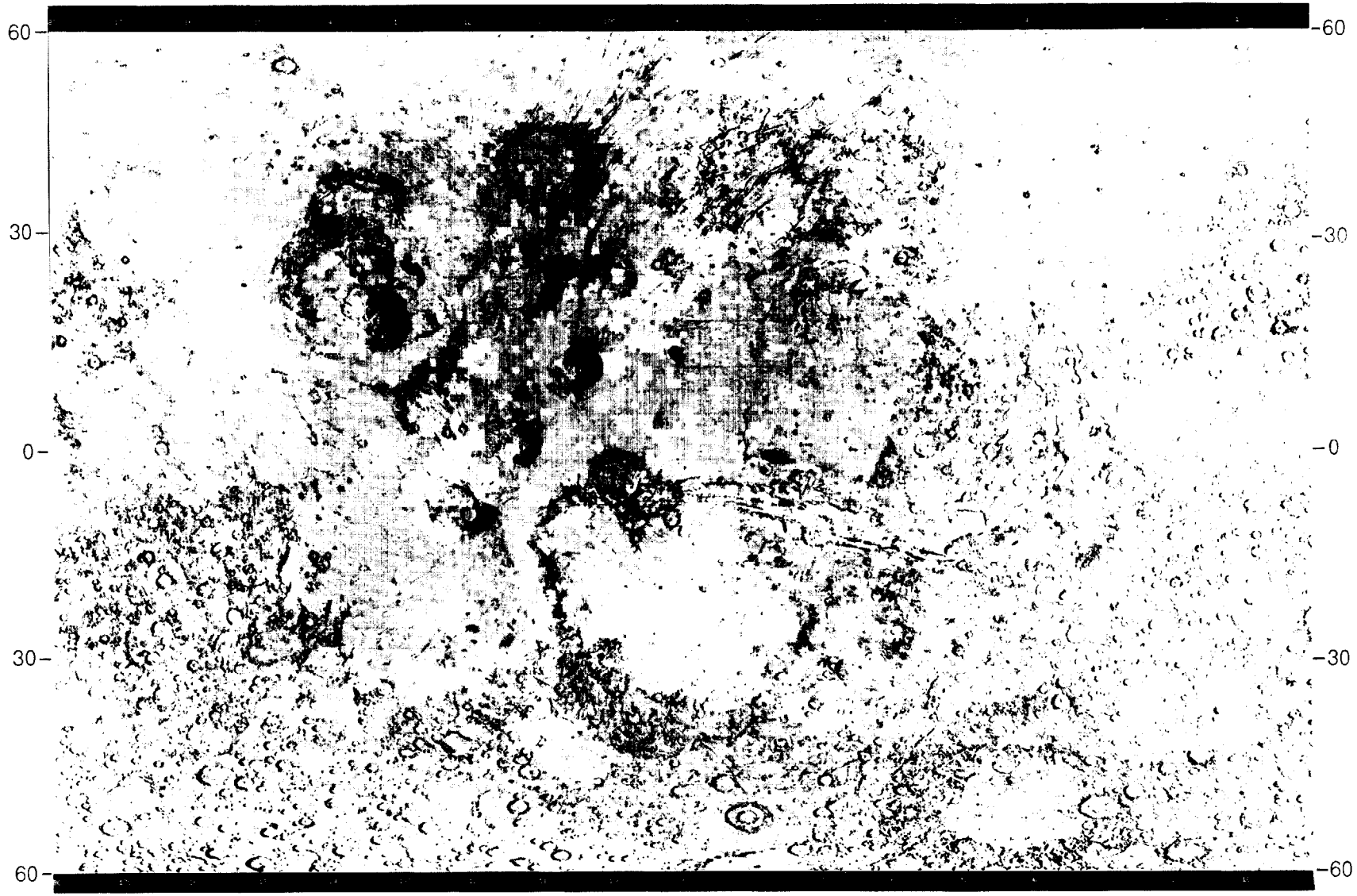

"Rock" abundance: 1 to 7% (dark grey), 8 to 14% (medium grey), > 14% (light grey)

ROCK ABUNDANCE ON MARS, EASTERN HEMISPHERE

(from Christensen, 1986)

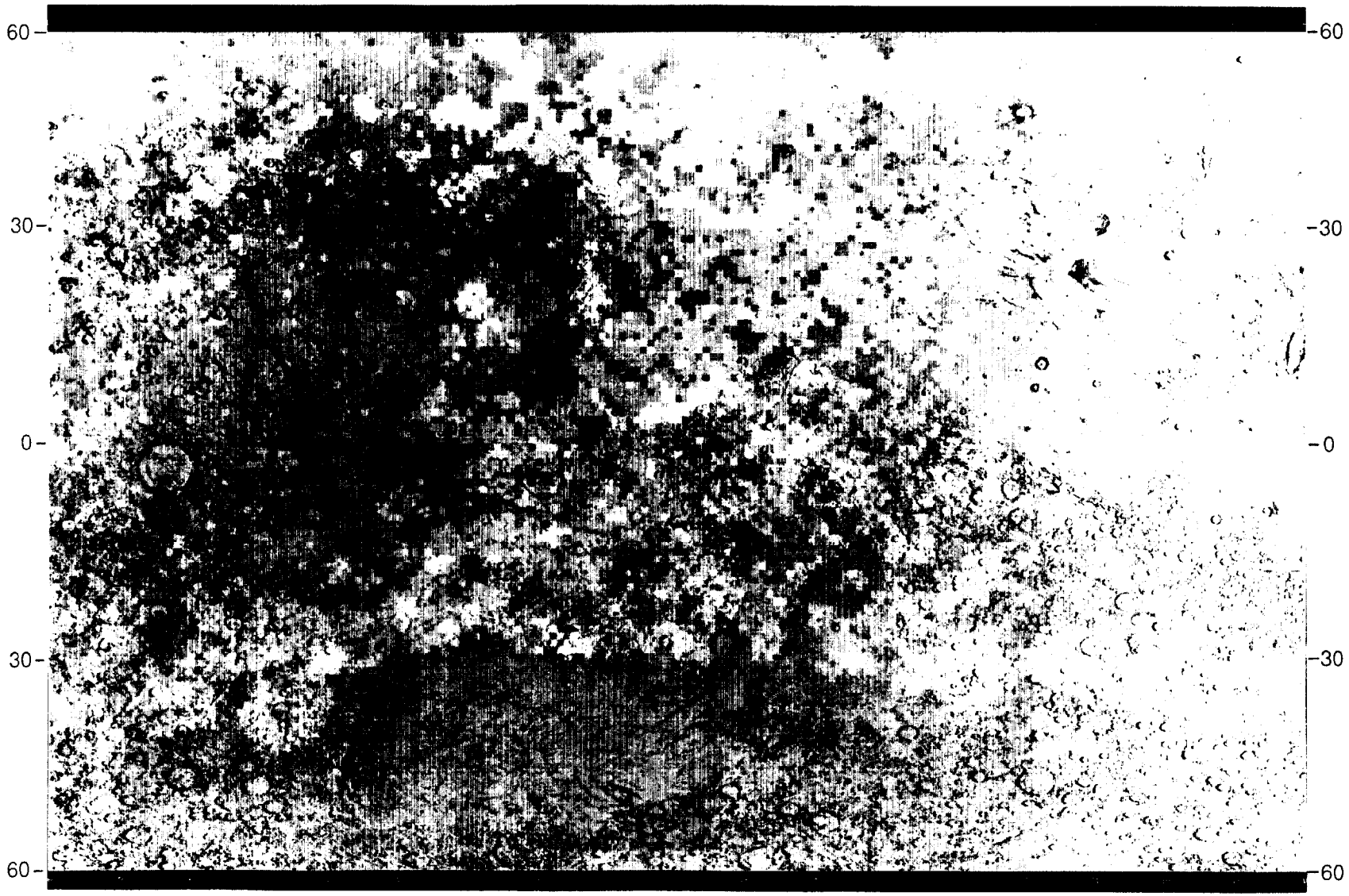

"Rock" abundance: 1 to 7% (dark grey), 8 to 14% (medium grey), > 14% (light grey)

MARS SURFACE UNIT MAP

(from Christensen and Moore, in press)

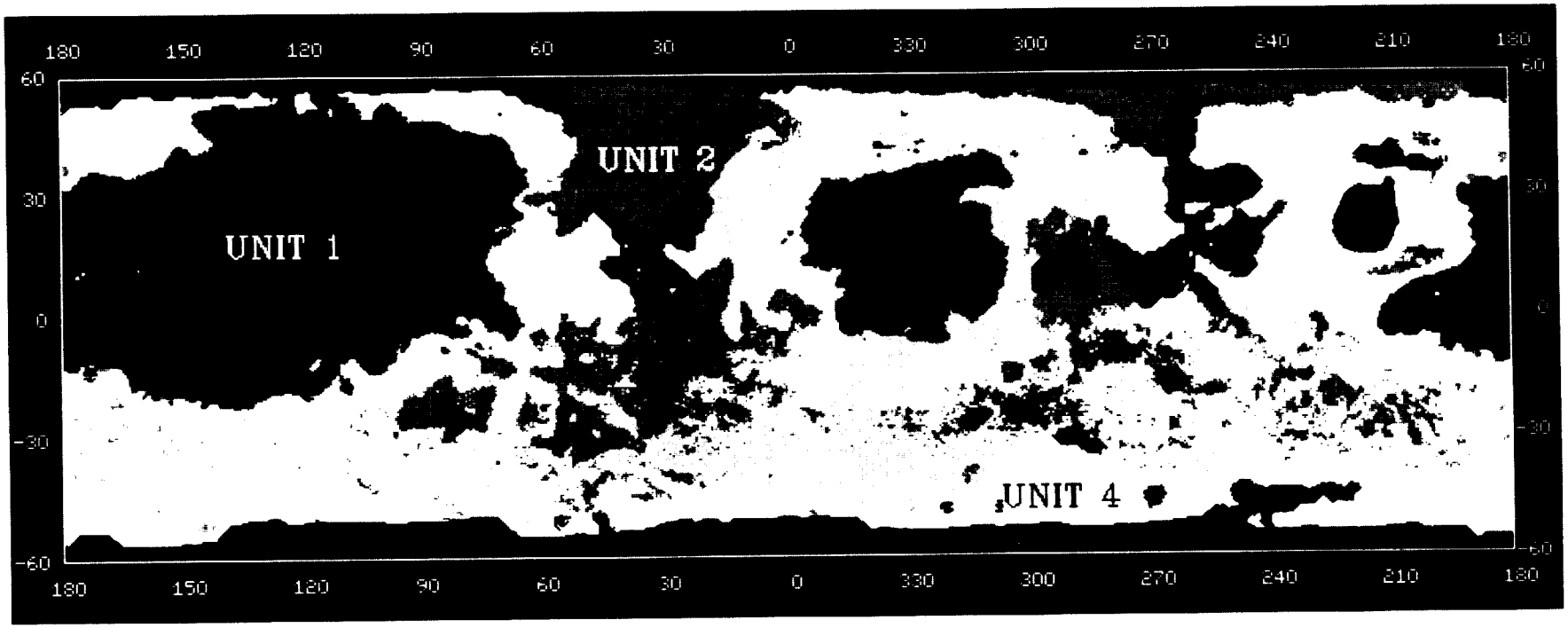

Unit 1: is covered by fine, bright dust that appears to be actively accumulating, with few rocks exposed at the surface. Radar observations of this unit indicate a very rough surface that is most likely buried beneath several meters of fine dust. This unit is interpreted to be a recent deposit, whose existence and extent may be linked to periodic climate changes.

Unit 2: is also active, with the motion of particles preventing dust accumulation and resulting in a dark, coarse surface with numerous rocks. Portions of this surface are mantled by sand to sufficient depth to bury nearly all surface rocks.

Unit 3: has intermediate inertia, albedo, and color, and is interpreted to be a rough, indurated surface over which other materials can be transported.

Unit 4: which contains both Viking landing sites, is characterized by relatively high inertia, but also has a high albedo, suggesting that dust may have accumulated, but has not reached sufficient thickness to affect the thermal properties.

Table 3. Supporting studies related to Sand and Dust on Mars

Mars Observations (to increase time-history of dust storms)

- HST
- Telescopic
- Radar observations/roughness mapping of Mars

Experiments (physical and chemical)

- Electrical properties, martian environment
  Paschen's curves
  Dust properties
- Chemical and physical behavior of particles < 1 μm
- Effects of all interparticle forces on grains < 60 μm
- Soil properties around Viking Landing sites
- Develop Mars soil analogs and assess development of duricrust
- Wind tunnel experiments of physics of sand and dust in martian environment
- Laboratory "bench tests" for Mars remote sensing observation
- Abrasion test (engineering) of materials under Mars conditions
- Engineering tests of solar panels in Mars environment
- Determine near surface particle threshold, velocity, and flux as function of surface roughness on Mars

Analyses

- Assess "threshold of significance" of Mars sand and dust from engineering perspective
- Develop software models of electrical properties
- Use of Mars soil and dust of source of water
- Refinement of General Circulation Model (smaller "bin size", etc.)
- Determine required height for wind measurements to characterize Mars near-surface boundary layer
- Develop sand and dust instrument "package" for Mars
- Develop models for sand and dust movement, to be tested in future observations (MOC, etc.)

Field Studies

- Develop/refine Mars analog sites for sand and dust
- Test results from experiments/analyses
- Develop more realistic (i.e., more complex!) scientific/engineering models for Mars

N91-27058

THE CHEMISTRY AND MINERALOGY OF MARS SOIL AND DUST. A. Banin, NRC/NASA Ames Research Center (MS 239-12), Moffett Field, CA 94305, and Hebrew University, Rehovot 76100, Israel.

A single "geological unit" consisting of fine, apparently weathered soil material is covering large portions of the surface of Mars. This soil material has been thoroughly homogenized by global dust storms and it is plausible to assume that Mars dust is strongly correlated with it.

The chemical-elemental composition of the soil has been directly measured by the Viking Landers. Positive detection of Si, Al, Fe, Mg, Ca, Ti, S, Cl and Br was achieved. Compared to most basalts, Fe is high and the MgO/Al_2O_3 ratio is uncommonly close to one. Potassium concentration is relatively low. Analyses of the SNC meteorites, a group of metorites that has been suggested to be ejected martian rocks, supply additional elemental-concentration data, broadening considerably our chemical data-base on the surface materials. A compositional model for Mars soil, giving selected average elemental concentrations of major and trace elements, was recently suggested (Table 1). It was constructed by combining the Viking Lander data, the SNC meteorite analyses, and other related analyses.

The mineralogy of the surface materials on Mars has not been directly measured yet. By use of various indirect approaches, including chemical correspondence to the surface anlayses, spectral analogies, simulations of Viking Lander experiments, analyses of the SNC meteorites and various modelling efforts, the mineralogical composition has been constrained to some extent. It is suggested that the fine surface materials on Mars are a multicomponent mixture of weathered and non-weathered minerals. Smectite clays, silicate mineraloids similar to palagonite, and scapolite, have been suggested as possible major candidate components among the weathered minerals. Iron is present as amorphous iron oxyhydroxides mixed with small amounts of crystallized iron oxides and oxyhydroxides, having extremely small particle sizes ("nanophases"). Specific candidate minerals that

have been proposed include nanophase hematite, lepidocrocite, goethite, and jarosite. As accessory minerals, it is likely that the soil contains various sulfate minerals, most probably calcium and magnesium sulfate, and chloride salts. If present, carbonates are likely to be at very low concentrations, although siderite ($FeCO_3$) may be present at somewhat higher concentrations. Organic matter is totally lacking.

No direct analyses of soil reactivity have been done yet. Indirect evidence, mostly from the Viking biology experimental results, suggests that the soil probably has a slightly acidic reaction (pH<7) and is generally oxidized. Upon humidification during the Viking biology experiments, the soil released oxygen and various other atmospheric gases. The amount of oxygen released was 70-770 nM/g. Whether the oxygen was physi-sorbed, present in peroxide or superoxide compounds, or both is not clear at present. Small particle size (nanophases) of both the silicate and the iron oxide minerals in the soil, may lead to high specific surface area and suggest potentially high catalytic reacitivty and high adsorption capacity of the soil.

Unambiguous identification of the Mars soil minerals by direct mineralogical analyses, and non-disturbed or *in situ* measurements of the soil's reactivity, are of primary importance in future Mars research.

Table 1

AVERAGE CHEMICAL COMPOSITION MODEL OF THE FINE MARTIAN SOIL

Constituent	Selected Average Concentration %	Constituent	Selected Average Concentration %	Constituent	Selected Average Concentration %
SiO_2	43.4*	K_2O	0.10**	SO_3	7.2*
Al_2O_3	7.2*	P_2O_5	0.68**	Cl	0.8*
Fe_2O_3	18.2*	MnO	0.45**		
MgO	6.0*	Na_2O	1.34**	CO_3	<2***
CaO	5.8*	Cr_2O	0.29**	NO_3	?
TiO_2	0.6*			H_2O	0-1+

* Based on direct soil analyses by Viking XRF.

** Based on SNC meteorite analyses.

*** Estimated from LR simulation.

\+ Varying content.

N91-27059

The Distribution of Particulate Material on Mars

Philip R. Christensen, Dept. of Geology, Arizona St. Univ., Tempe, AZ 95287

The surface materials on Mars have been extensively studied using a variety of spacecraft and Earth-based remote-sensing observations (1-7). These measurements include: 1) diurnal thermal measurements, used to determine average particle size, rock abundance, and the presence of crusts; 2) radar observations, used to estimate the surface slope distributions, wavelength-scale roughness, and density; 3) radio emission observations, used to estimate subsurface density; 4) broadband albedo measurements, used to study the time variation of surface brightness and dust deposition and removal; and 5) color observations, used to infer composition, mixing, and the presence of crusts. Remote sensing observations generally require some degree of modeling to interpret, making them more difficult to interpret than direct observations from the surface. They do, however, provide a means for examining the surface properties over the entire planet and a means of sampling varying depths within the regolith. Albedo and color observations only indicate the properties of the upper-most few microns, but are very sensitive to thin, sometimes emphemeral dust coatings. Thermal observations sample the upper skin depth, generally 2-10 cm. Rock abundance measurements give an indirect indication of surface mantling, where the absence of rocks suggests mantles of several meters. Finally, radar and radio emission data can penetrate several meters into the surface, providing an estimate of subsurface density and roughness.

For an assumed smooth, homogeneous surface, the average particle size can be determined from the thermal inertia using diurnal temperature measurements (3). For typical geologic materials in the martian environment, thermal inertia is primarily controlled by the thermal conductivity. Variations in conductivity are due to differences in particle size, porosity, or the degree of bonding, with laboratory measurements providing the link between thermal inertia and these parameters (8). Conductivity, density, and therefore thermal inertia, are lowest for small particles with small cohesion, such as loose dust, and highest for solid rock. It is important to note, however, that thermal inertia is a bulk property, such that unimodal, medium sand, a mixture of fine sand and pebbles, or crusted fines could all have identical thermal inertias.

Some of the ambiguity in thermal inertia can be resolved by incorporating multi-wavelength thermal observations to resolve the surface materials into fine and rock components. This modeling is based on the fact that the temperatures of high-thermal-inertia rocks and low-thermal-inertia fines differ by up to 60 K at night. The energy emitted from a surface of materials at different kinetic temperatures is not blackbody in nature, and the observed thermal spectrum can be inverted to determine the fraction of the surface covered by each temperature component. To keep the number of free parameters in this model small, yet provide useful surface information, only two components are assumed: rocks (~10-15 cm in diameter and larger) and fines. This model is only weakly sensitive to the exact size of the rocks, and provides an estimate of the total fraction of the surface covered by rocks greater than 10 cm in diameter.

Thermal data reveal the presence of large low- and high-inertia regions in the northern hemisphere, with much of the south covered by material of moderate inertia. Substantial regions in Tharsis and Arabia appear dust covered, suggesting active accumulation of deposits 1-2 m thick (6). Results from the rock modeling indicate that the modal surface rock cover is 6%, with abundances ranging from several percent to ~35%. The rock abundances of the regions surrounding the Viking 1 and 2 landing sites, determined from this model, are ~10% and 20% respectively, in good agreement with the rock abundances observed from the landers, as discussed previously. Thus, in retrospect, it can be seen that both sites have above average rock abundances, and the VL2 site is one of the rockiest regions on the planet.

Radar observations of Mars from Earth and from Mars orbit provide information on surface reflectivity and dielectric constant, and fine-scale roughness on a scale of the radar wavelength and smaller. The reflectivity may be used to estimate the dielectric constant (ε) of the surface materials (e.g. 10). Variations in ε are primarily due to changes in the bulk density of the surface, with lower density material generally having a lower ε and lower reflectivity . Downs et al. (10) reported an

"average" reflectivity for Mars of 6.4% based on an extensive series of measurements in the south equatorial region (14-22° S). They noted considerable variation, however, in particular the extremely low reflectivities in Tharsis and the region to the west, corresponding to densities of approximately 1.5 g/cm^3, consistent with powdered rock values, and high values (ε=4) in Syrtis Major (11) , suggesting the presence of solid rock at the surface.

That part of the radar echo that can not be attributed to mirror-like reflection from large facets is called the "diffuse" component. It arises from scattering by irregular structure in the surface, perturbations on the facets, and from multiple scattering, typically at scales of 0.3 to 3 times the radar wavelength. This scattering results in a depolarized echo in addition to the quasi-specular, polarized return. Dual-polarization radar observations at 12.6 cm have detected the diffuse reflection, with a concentration of data in the Tharsis region at 20-25° N. These data indicate that the Tharsis region has very large concentrations of surface to near surface roughness elements (12). These observations appear to conflict with the thermal results, but can be reconciled by a model of high-radar-reflecting rocks buried by 1-2 m of dust.

Albedo observations have been used to study the composition, particle size, packing, porosity, and macroscale roughness of the uppermost microns of the surface using broadband Viking IRTM reflectance measurements (4). IRTM observations have also been used to determine the spatial and temporal variations of the albedo of the martian surface and atmosphere throughout the Viking mission (4,8). The northern hemisphere atmosphere was dustier during storms, consistent with south-to-north transport of dust. Northern-hemisphere dark regions were also brighter following the storm, indicating the deposition of ~7 to 45 μm of dust per year. These surfaces subsequently darkened over the following months, suggesting active removal of material.

On a global basis there is a strong anticorrelation between inertia and albedo, a correlation between inertia and rock abundance, and, over much of the planet, a correlation of radar-derived density with inertia (13). The correlation between density and inertia might be due to the presence of subsurface crusts which would simultaneously increase both of these properties. Viking Orbiter color data indicate the presence of three major surface materials: low-inertia, bright-red material that is presumably dust; high-inertia, dark-grey material interpreted to be lithic material mixed with palagonite-like dust; and moderate-inertia, dark-red material that is rough at sub-pixel scales and interpreted to be indurated. Observations from the Viking landing sites show rocks, fines of varying cohesion, and crusts. These sites have indications of aeolian erosion and deposition in the recent past. Large rocks have been exhumed from beneath fines, suggesting one or more cycles of deposition and erosion. Taken together, the remote and *in-situ* data suggest that much of the surface can be characterized by four basic units. Unit 1 is covered by fine, bright dust, with few rocks exposed at the surface. Radar observations indicate that much of this unit is very rough, suggesting a rough surface that is mostly buried beneath several meters of fine dust. This unit may be a recent deposit, whose location may be linked to periodic climate changes. Unit 2 is also active, with the motion of particles keeping the surface free of dust, resulting in a dark, coarse-grained surface with abundant rocks. Unit 3 has intermediate inertia, albedo, and color, and is interpreted to be a rough, indurated surface. Unit 4 is a relatively minor unit, but it contains both Viking landing sites. It is characterized by relatively high inertia and high albedo, suggesting that a thin layer of dust may have accumulated. The landing sites appear to be representative of the types of processes that have occurred globally, but are not completely representative of the major units. They have not accumulated significant amounts of dust, nor are they experiencing active transport and erosion by sand-sized particles. Crusts are present, but not to the degree that may be present elsewhere. Numerous, recently-active processes are inferred from the surface characteristics, including dust deposition, erosion, aeolian transport and sorting, and crust formation. The available data suggest that cyclic changes in sedimentary processes may occur over several timescales associated with periodic climate changes. Large dust deposits presently occur in the north, with maximum winds and dust storm activity in the south. Under different environmental conditions these deposits may be eroded and transported elsewhere. Much of the present surface appears young and may have been continually reworked. The continued erosion and redeposition of this loose material, rather than erosion of fresh surfaces, may provide the material for the high

rates of aeolian activity. As a consequence, much of the fine material on the surface may have been globally homogenized and essentially decoupled from the underlying bedrock.

Perhaps the most the most significant conclusion that can be drawn from our current understanding of the upper layer is that much of the present surface is young and has been continually reworked. The continued erosion and redeposition of this loose material, rather than erosion of fresh surfaces, may provide the material for the high rates of aeolian activity. As a consequence, much of the fine material on the surface may have been globally homogenized and may be essentially decoupled from the underlying bedrock.

REFERENCES

1) Kieffer, H.H., Martin, T.Z., Peterfreund, A.R., Jakosky, B.M., Miner, E.D., and Palluconi, F.D., 1977, *J. Geophys. Res.*, *82*, 4249-4292. 2) Arvidson, R.E., Guinness, E.A., Dale-Bannister, M.A., Adams, J., Smith, M., Christensen, P.R., and Singer, R.B., 1989, *J. Geophys. Res.*, *94*, 1573-1587. 3) Palluconi, F.D., and Kieffer, H.H., 1981, *Icarus*, *45*, 415-426. 4) Pleskot, L.K., and Miner, E.D., 1981, *Icarus*, *45*, 179-201. 5) Christensen, P.R., 1986a, *Icarus*, *68*, 217-238. 6) Christensen, P.R., 1986b, *J. Geophys. Res.*, *91*, 3533-3546. 7) Zimbelman, J.R., and Leshin, L.A., 1987, *J. Geophys. Res.*, *92*, E588-E586. 8) Christensen, P.R., 1988, *J. Geophys. Res.*, *93*, 7611-7624. 9) Wechsler, A.E., and Glaser, P.E., 1965, *Icarus*, *4*, 335-352. 10) Downs, G.S., Goldstein, R.M., Green, R.R., Morris, G.A., and Reichley, P.E., 1973, *Icarus*, *18*, 8-21. 11) Simpson, R.A., Tyler, G.L., Harmon, J.K., and Peterfreund, A.R., 1982, *Icarus*, *49*, 258-283.12) Harmon, J.K., Campbell, D.B., and Ostro, S.J., 1982, *Icarus*, *52*, 171-187. 13) Jakosky, B.M., and Muhleman, D.O., 1981, *Icarus*, *45*, 25-38.

N91-27060

RECENT STUDIES OF THE OPTICAL PROPERTIES OF DUST AND CLOUD PARTICLES IN THE MARS ATMOSPHERE, AND THE INTERANNUAL FREQUENCY OF GLOBAL DUST STORMS

R. T. Clancy and S. W. Lee, LASP, Univ. of Colorado, Boulder, CO 80309, and D. O. Muhleman,Caltech, Pasadena, CA 91125

The results of research with two distinctly separate sets of observations yield new information on the optical properties of particulate scatterers in the Mars atmosphere, and on the interannual variability of the abundance of such scatterers in the Mars atmosphere. The first set of observations were taken by the IRTM (Infrared Thermal Mapper) instrument onboard the Viking orbiters, during the period 1976-1980. Several hundred emission-phase-function (EPF) sequences were obtained over the Viking mission, in which the IRTM visual brightness channel observed the same area of surface/ atmosphere as the spacecraft passed overhead. The 1-2% accuracy of calibration [1] and the phase-angle coverage that characterizes these data make them ideally suited to determining both the optical depths and optical properties of dust and cloud scatterers in the Mars atmosphere versus latitude, longitude, season (L_s), and surface elevation over the extended period of Viking observations. The range of seasons and locations for these observations are indicated in figure 1, in which the dust optical depth over regions from 19 separate EPF sequences are plotted versus L_s. [2] Mars cloud opacities are presented in figure 2. We have analyzed the EPF data with a multiple scattering radiative transfer code [3] to determine dust single scattering albedos which are distinctly higher (0.92 vs 0.86) than indicated by the Viking lander observations [4]. Although we find a single scattering phase function that is very consistent with that returned by the Viking lander observations, the scattering asymmetry parameter is 0.55 rather than the value of 0.79 reported by Pollack et al. [4]. These differences in the optical properties of atmospheric dust lead to very different radiative properties, and suggest much smaller particle sizes than previously considered (effective radius $\leq$0.4 μm vs 2.5 μm). Implications regarding dust heating of the atmosphere, dust settling times, opacity ratios between visible and infrared wavelengths, and the dust-corrected albedos of the Mars surface are considered.

The second set of observations regard ground-based observations of the 1.3-2.6 mm rotational transitions of CO in the Mars atmsophere. We have derived the low-to-mid latitude average of the atmospheric temperature profile (0-70 km altitude) from a number of such observations over the 1980- 1990 period [5]. A comparison of these microwave temperatures with those inferred from the Viking lander descent and orbiter IRTM observations (figure 3) indicates a distinct difference. The microwave temperatures are ~20 K cooler at all altitudes, and are consistent with radiative-convective equilibrium temperatures for the Mars atmosphere in the absence of significant dust heating [6]. Implications concerning the relative infrequence of global dust storms over the 1980-1990 period, the enhanced frequency of clouds expected with such colder atmospheric temperatures, and the accompanying changes in the atmospheric density profile are presented.

REFERENCES: [1] Pleskot, L.K., and E.D. Miner (1981). Time variability of martian bolometric albedo. *Icarus* 45, 179-201. [2] Clancy, R.T., and S. W. Lee (1991) A new look at dust and clouds in the Mars atmosphere: an analysis of emission-phase-function sequences from global Viking IRTM observations, *Icarus*, in prepartion, [3] Stamnes, K., S.C. Tsay, W. Wiscombe, and K. Jayaweera (1988). A numerically stable algorithm for discrete-ordinate-method radiative transfer in scattering and emitting layered media. *Appl. Opt.*, 27, 2502-2509. [4] Pollack, J.B., D.S. Colburn, F.M. Flasar, R. Kahn, C.E. Carlston, and D. Pidek (1979), Properties and effects of dust particles suspended in the martian atmosphere, J. *Geophys. Res.*, 84, 2929-2945. [5] Clancy, R.T., D.O. Muhleman, and G.L. Berge (1990). Global changes in the 0-70 km thermal structure of the Mars atmosphere derived from 1975-1989 microwave Co spectra, *J. Geophys. Res.*, 95, 14543-14554. [6] Gierasch, P.J. and R.M. Goody (1968). A study of the thermal and dynamical structure of the Martian lower atmosphere, *Planet. Space Sci.*, 16, 615.

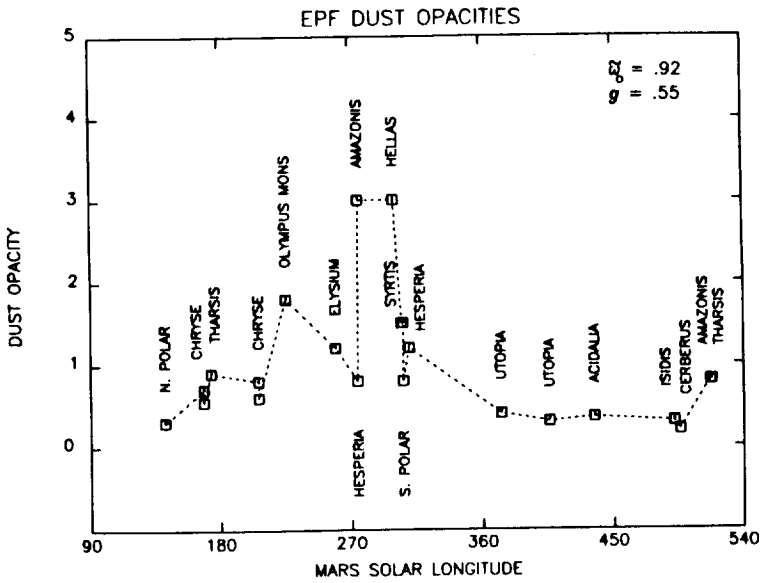

Figure 1. The dust extinction opacity (broadband solar) plotted versus solar longitude, as measured from Viking IRTM EPF data at various regions on Mars. The two global dust storms of 1976-1977 are apparent as L_s near 200-300°.

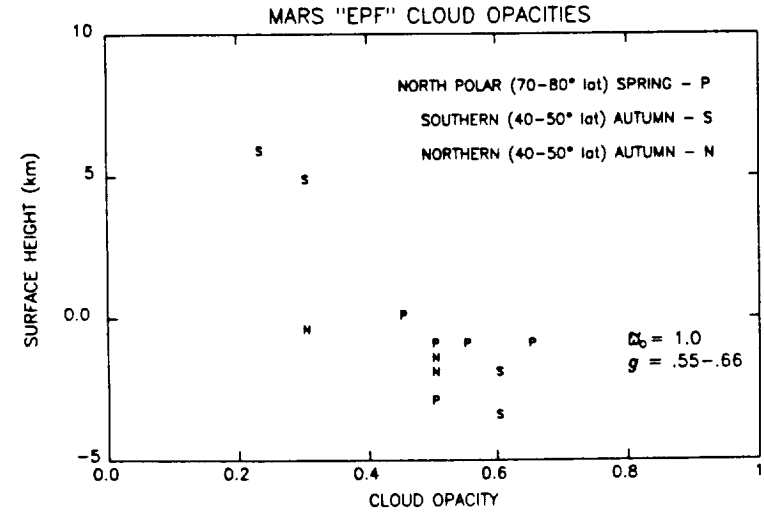

Figure 2. Extinction cloud opacities determined from the Viking IRTM EPF observations, plotted versus the surface elevation of the observed region. The various regions and seasons of these clouds are distinguished by different symbols.

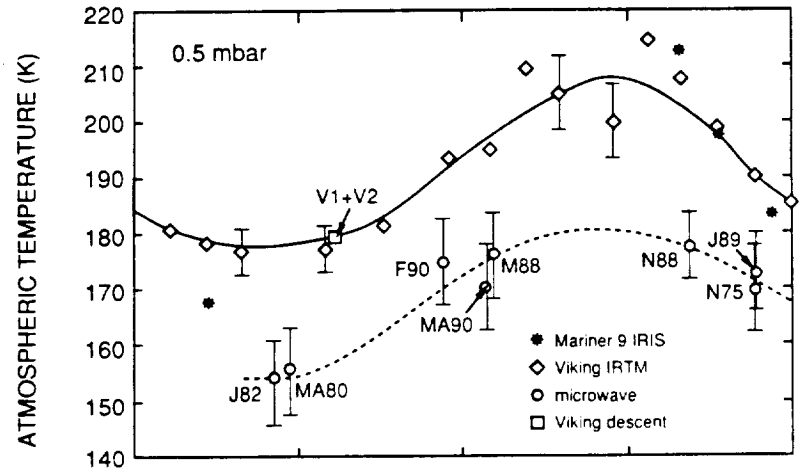

Figure 3. The low-to-mid latitude average temperature of the 0.5 mbar (~25 km) pressure level of the Mars atmosphere is plotted versus Mars season (L_s). The measurements connected by a solid line are obtained from Viking lander descents, Viking IRTM infrared temperatures, and Mariner 9 IRIS spectra; and correspond to high dust loading in the Mars atmosphere. The ground-based microwave measurements (circles) are connected by a smooth dashed line to indicate the seasonal dependence of atmospheric temperatures presumably related to low-dust loading in the Mars atmosphere. The month and year of the microwave measurements are indicated (M88=May, 1988).

EFFECTS OF MARTIAN DUST ON POWER SYSTEM COMPONENTS

J.R. Gaier, M.E. Perez-Davis, NASA Lewis Research Center

Manned exploration of the Martian surface as envisioned by the Space Exploration Initiative proposed by President Bush in 1989 will require large amounts of power. In contrast to the Viking landers, which used about 70 watts of power, most scenarios of a manned Martian mission envision power systems generating hundreds of kilowatts. Radioisotope thermal generators (RTG's) which were so successful in providing the Viking landers with power, will have to be supplanted with larger power systems based on large photovoltaic arrays coupled to regenerative fuel cells or with nuclear reactors. Before these large power systems can be put into place, it must be determined how their performance will be affected by the Martian environment.

There are several hostile elements within the Martian environment which have the potential to degrade the power system. These include wide daily temperature swings (up to 50 K), ultraviolet radiation, high energy particle radiation, high velocity winds (albeit at low pressure), chemically reactive species in the soil, atmospheric condensates, and dust storms. At NASA Lewis we have initiated a program to assess the impact of these environmental factors on power system performance. It is also part of our goal to find ways to mitigate these degradative effects.

The effects of blowing dust on photovoltaic (PV) and radiator surfaces is the subject of our initial work. In this work we have made extensive use of the Martian Surface Wind Tunnel (MARSWIT) located at NASA Ames Research Center to simulate Martian winds. To date we have run two basic types of experiment sets. In the first, we have studied the threshold clearing velocity of dust deposited on PV coverslip materials and high emissivity radiator materials in clear Martian-like winds. In the second, we have dropped dust near the inlet of the wind tunnel and allowed the winds to carry the dust past the samples, simulating a dust storm. Below is a summary of our results.

In order to test the ability of the wind to remove dust from surfaces, dust must first be deposited on those surfaces. In order to most closely simulate the way that dust would deposited on a surface after a storm, a dust deposition box was constructed. The box has three principle components, an inverted square pyramidal base, a 1 meter high upper chamber, and a sliding drawer. A quantity of dust is first placed in the bottom of the inverted pyramid. A blast of dried air is directed downward onto the dust with sufficient force to elevate the dust into the upper chamber. The air is then turned off and the dust allowed to settle out. Stokes law tells us that large particles will fall the fastest, so for the first 15 seconds the larger particles and conglomerates are allowed to fall back into the inverted pyramid. The drawer holding the samples is then slid into the path of the falling dust so that the fine particles settle onto the sample holder. See NASA CP-3096 (1990) p. 447, for additional information.

Three different types of dust were used. In the initial experiments, an aluminum oxide based optical polishing grit with a size range of 1.5 to 30 μm was used. This material does not easily form agglomerates in air and so was easy to work with. In later experiments a basaltic dust of the same approximate size was used because its chemistry is similar to that of Martian dust. Finally, very fine grained (0.3 to 3 μm) ferric oxide powder was used.

In the first series of tests, optical polishing grit was deposited six different types of PV coverslips and three different types of high emittance radiator surfaces. The height from the MARSWIT floor, angle of attack, and wind velocity were all varied in an attempt to determine the important parameters. It was found using optical transmittance that the PV coating material and height from the MARSWIT floor were only minor influences in the clearing of dust from these surfaces. Angle of attack and wind velocity were found to be

the major influences. The wind velocities of 55, 85, and 124 m/s were found to be sufficient to clear most of the dust off of the PV surfaces within a few minutes.

In the second series of tests, lower velocity winds were used (10, 30, and 35 m/s). At 10 m/s, virtually no clearing occurred. A small amount of clearing occurred during the 30 m/s test, and considerably more at 35 m/s. The threshold value varies with angle of attack, and at 45°, that value is near 35 m/s. The clearing dropped both at lower and at higher angles. In those samples where the dust removal was incomplete it was noted that the dust appeared to be lifted directly upward from the surface. This seems to implicate and aerodynamic lift mechanism which plucks the dust particles directly off of the surface before the wind stream carries it off. Evidence was also found for a second dust removal mechanism. At lower velocities the dust left streaks in the wind direction, indicating perhaps that the dust particles "roll" along the surface for a short distance before they are lifted up into the wind. Evidence for this was seen only in the low angle (22.5°) sample. During the second set of tests a turbulence fence was introduced with the idea to induce clearing at lower wind velocities by providing regions of high local velocity. However, it was found that the turbulence fence actually raised the threshold clearing velocity instead of lowering it. These experiments are summarized in NASA TM-102507 (1990).

The goal of the third series of tests was to examine the sensitivity of the threshold clearing velocity to the composition of the dust. Thus, in addition to the optical polishing grit, basalt and ferric oxide dusted samples were placed in the MARSWIT. The threshold clearing velocity of the basalt was very similar to the optical polishing grit, ranging between 30 and 40 m/s for a 45° angle. The threshold clearing velocity for the ferric oxide was much higher (between 85 and 95 m/s), but it is unclear how much of the effect is due to chemistry and how much is due to particle size effects. These two samples did, however, confirm that the optimum angle for dust clearing is something near 45°. It appeared from these tests that of the two dust removal mechanisms that the "rolling" mechanism has a lower threshold velocity, but that the "aerodynamic" mechanism is more efficient and so dominates at higher velocities. Degradation of the emittance of radiator surfaces was also observed. It was found that ion beam textured graphite and carbon-carbon composite samples degraded less that did arc-textured copper or niobium-1%-zirconium. This was due to the abrasion of the carbon from the surface of the arc-textured metal samples, which lowered their emittance appreciably. The radiator work is reported in NASA TM-103205 (1990), and PV work in NASA CP-3096 (1990) p. 379.

The fourth test series examined the effects of blowing dust on PV and radiator surfaces. It was found that exposure to dust laden wind changed the dust clearing behavior of the samples. Initially clean samples became dusty even when they were exposed to winds well above the threshold clearing values (97 m/s). Initially dusted samples partially cleared well below the threshold velocity (19 m/s). Samples tended to converge to an equilibrium dustiness independent of their initial condition, but dependant upon the wind velocity. It was found that abrasion was much more of a problem with both arc-textured metals, and glass coverslips. Interestingly, it was found that an initial coating of dust actually reduced the amount of abrasion, at least in the case of arc-textured radiator samples. NASA TM-103704 (1991) summarizes this work.

The most important information we have learned to date is that interactions between the wind-blown dust on Mars and power system components are complex. We do not yet have answers even to the extent of the problem. The results of these types of tests have far-ranging implications for the design of the power system, and thus this work needs to be performed during the early stages of system design.

HAVE GRABEN WALL SCARPS ACCUMULATED SAND AND DUST ON MARS?

M. P. Golombek[1] and P. A. Davis[2], [1]Jet Propulsion Laboratory, Caltech, Pasadena, CA, 91109, [2]U. S. Geological Survey, Flagstaff, AZ 86001.

Grabens are linear fault bounded troughs that are extremely abundant on Mars (about 7000 cover the western hemisphere). Their dimensions are variable, but commonly are a few kilometers wide, a hundred meters deep and tens to hundreds of kilometers long. In their simplest form, grabens have flat floors, parallel bounding scarps of equal width (and height), flat shoulders at equal elevations, and extend for many kilometers in length with only small changes in width. In surface appearance and morphology many look fresh and unmodified.

Analysis of lunar and martian grabens as well as analogous structures on Earth indicates that grabens form under extension when the crust is pulled apart. The graben accommodates the extension by slip along inward dipping normal faults that allow the floor of the graben to drop. Measurement of the increase in width of simple grabens over local regions of high relief on the Moon (e.g., 1) and observations of the trace of faults bounding grabens where they intersect the walls of steep troughs on Mars (2) shows that faults bounding grabens dip at about 60°. Nevertheless the slopes of graben wall scarps are substantially shallower than this. On the Moon, measurement of graben wall slopes (1), where high resolution topographic maps exist (Lunar Topographic Orthophotomaps), shows slopes of 15-23° (average of 18° for 17 determinations). It is not clear how graben scarps weather from their initial steep slopes to slopes lower than the angle of repose (about 30° for unconsolidated material applicable to the outer layers of the Moon). A possible explanation is mass wasting by seismic shaking and impact by micrometeorites. Mass wasting involves unconsolidated material along the top of the scarp sliding and crumbling down the graben walls thereby reducing the slope down to the angle of repose. Micrometeorite bombardment could be responsible for reducing angle of repose slopes to those observed.

On Mars topographic maps are not of sufficient resolution to measure graben wall slopes. However, about 150 measurements have been made using photoclinometry, a technique based on pixel brightness variations along a profile being due to topographic relief (assuming the albedo is constant), which has been shown to be accurate to within 15% over areas of local relief (e.g., 3). Results show low slopes of 7-11° (2, 3), with an average of 9° or about half that of lunar graben scarps. Even if there is a factor of 2 uncertainty in the slopes they are still well below the angle of repose expected simply from mass wasting and micrometeorite bombardment cannot be appealed to on Mars. Although the cause of such low slopes is not known, the deposition of sand and dust is a possible explanation.

Seismic shaking on Mars might be capable of reducing 60° fault scarps to the angle of repose. Some other process must be responsible for further reducing graben wall slopes. Whatever process this is, it has not altered the fresh appearance and simple symmetric profile observed at the resolution of the Viking images. This seems to rule out water driven processes such as sapping or runoff (erosion), as such processes would not preserve the parallel linear scarp edges across the structure, but would tend to scallop out and further make the edges irregular, which is not observed. In contrast the deposition of sand and dust along graben walls might be capable of producing a smooth even scarp of low slope.

If the deposition of sand and dust along graben walls is responsible for their extremely low slopes, then a variety of implications are possible. Sand and/or dust movement and deposition is ubiquitous in grabens over most of Mars, as similar looking grabens are found over the entire western hemisphere and this requires a plentiful supply of sand or dust. If the material that accumulates is of low density and cohesion, attempts to traverse graben walls might be difficult. Finally, rimless shallow depressions could be more effective sinks for sand and dust on Mars than has been realized.

References:

(1) Golombek, M. P., Jour. Geophys. Res., v. 84, p. 4657-4666, 1979.
(2) Davis, P. A., and M. P. Golombek, Jour. Geophys. Res., v. 95, p. 14,231-14,248, 1990.
(3) Tanaka, K. L., and P. A. Davis, Jour. Geophys. Res., v. 93, p. 14,893-14,917, 1988.

N91-27063

CHEMISTRY AND MINERALOGY OF MARTIAN DUST: AN EXPLORER'S PRIMER

James L. Gooding, SN21/Planetary Science Branch, NASA/Johnson Space Center, Houston, TX 77058

Introduction. A summary of chemical and mineralogical properties of Martian surface dust is offered for the benefit of engineers or mission planners who are designing hardware or strategies for Mars surface exploration. For technical details and specialized explanations, reference should be made to the literature cited. We have four sources of information about Martian dust composition:

(1) Experiments performed on the Mars surface by the *Viking* Landers (*VL*) 1 and 2 (1976-1978) and Earth-based laboratory experiments attempting to duplicate those results [1];
(2) Infrared spectrophotometry remotely performed from Mars orbit, mostly by *Mariner 9* (1971-72) [2] and to be continued with *Mars Observer* (*MO*; 1992 launch);
(3) Visible and infrared spectrophotometry remotely performed from Earth [3];
(4) Laboratory studies of the shergottite-nakhlite-chassignite (SNC) clan of meteorites (since 1985) [4], for which compelling evidence suggests origin on Mars.

Source (1) is limited to fine-grained sediments at (or a few centimeters below) the surface (no rock analyses were possible) whereas (2) and (3) contain mixed information about surface dust (and associated rocks) and atmospheric dust. Source (4) has provided surprisingly detailed information but investigations are still incomplete.

Chemical Composition. Each *VL* carried a gas chromatograph/mass spectrometer (GCMS) and X-ray fluorescence spectrometer (XRFS) that produced information on the elemental composition of fine-grained surface sediments. The GCMS found no organic matter (for detection limits of a few parts per billion (ppb) to a few parts per million (ppm) by weight) but revealed water and adsorbed gases. Volatile inorganic compounds were not precisely measured except to bracket concentrations of 0.1-1 (and possibly as high as 3) wt. % H_2O and 50-700 ppm CO_2 in the sediments. Better measurements must be left to future experiments.

The XRFS found iron-rich sediments with surprisingly high concentrations of sulfur and chlorine (Table 1); virtually identical compositions at the two widely separated landing sites implied that the surface sediments represent homogenized, windblown dust. Unfortunately, the XRFS was not sensitive to several important chemical elements (including carbon, nitrogen, and sodium) and had comparatively large uncertainties for others. In addition, XRFS, as a method, is not capable of identifying the ways in which elements are combined as compounds. Therefore, our direct knowledge of chemical composition of sediments remains incomplete.

Precise analyses of more than 60 elements in SNC meteorites have been used to prepare detailed, if somewhat conjectural, compositional models for Martian rocks. Nonetheless, it is still not clear how these models might pertain to the dust, which is almost certainly more complex than pulverized volcanic rocks.

The *MO* gamma ray spectrometer (GRS) experiment will map the abundances of about 18 chemical elements from Mars orbit but its spatial resolution (footprint size) on the surface will be a few hundred kilometers. Also, the GRS emphasizes the search for variations rather than the precise numerical measurement of concentration values; GRS data will supplement but not supplant *VL* XRFS data.

Mineral Composition. None of the *VL* experiments were capable of directly identifying minerals; conclusions about minerals rest on inference only. The surface sediments apparently contain 1-7 wt. % of a strongly magnetic material which is probably a ferric (iron) oxide. Laboratory simulations of *VL* biology results (see below) are consistent with (but do not prove) presence of iron-rich clays of the smectite mineral family. Remote-sensing spectrophotometry favors a material denoted as "palagonite" which, on Earth, forms by natural water-driven weathering of volcanic glasses produced by basaltic (Hawaiian-type) volcanoes. Much of the favorable comparison between remotely sensed Mars spectra and laboratory spectra for palagonite is attributable to an ultrafine-grained ferric oxide known as nanophase hematite.

The *Mariner 9* infrared radiometer interferometer spectrometer (IRIS) observed the Martian atmosphere during various stages of dust storm activity. No firm mineral identifications were achieved but the suspended dust was inferred to be mostly silicon-oxygen-based minerals such as clays or feldspars. Although surface dust is undoubtedly related to high-altitude atmospheric dust, the IRIS results for atmospheric dust can explain only a portion of the surface dust as characterized by the XRFS. The *MO* thermal emission spectrometer (TES) will map minerals from Mars orbit at a surface resolution of about 3 km/pixel but will emphasize global and regional differences rather than exact and comprehensive mineral identifications.

Weathering products in SNC meteorites might represent our current best view of minerals most likely to form Martian dust. Although SNC meteorites are volcanic products, they contain traces of minerals that clearly formed in oxidizing, watery environments of the types we might expect at the Mars surface. The minerals provisionally identified (Table 2) include iron-rich, clay-like materials and sulfur- and chlorine-bearing salts that are entirely consistent with the bulk elemental compositions of Martian sediments as measured by the *VL* XRFS; the carbonate minerals in SNCs would not have been detected by either the GCMS or XRFS. Precise identification of these tiny mineral grains (most < 20 μm size) remains an active area of research from which further significant conclusions are expected.

Chemical Reactivity and Corrosivity. The three different microbiological life-detection experiments on each *VL* produced apparently "positive" results that were eventually interpreted as the action of vigorously reactive inorganic compounds (rather than microbial life). These agents evolved oxygen when wetted with water, oxidized simple organic compounds in water-based solution, and fixed carbon dioxide into a form that was non-volatile under ambient Martian conditions. The *VL* experiments were incapable of identifying the reactive agents although, through Earth-based simulation experiments, they were variously inferred to be metal peroxides or superoxides, alkali peroxonitrites or catalytically active minerals (such as clays or iron oxides). Although their actions were striking, their concentrations were quite low: perhaps 1 ppb to a few tens of ppm when expressed in terms of reactivity equivalent to hydrogen peroxide. Although further analyses are important, it appears that at least one of the reactive agents can be decomposed by simple treatment with water.

Over nearly three Martian years of observations, no obvious corrosion of the *VL*s was observed. Mars dust wetted with water might become electrochemically corrosive toward metals if the sulfur and chlorine in the dust occur as salts (as the SNC evidence suggests) but only further experiments will constrain the possibilities.

Toxicity. None of the *VL*, laboratory, or remote-sensing results can be used to make blanket statements about toxicity or non-toxicity of Martian dust. Neither the VL XRFS data nor the extensive analyses of SNC meteorites has revealed unexpected concentrations of heavy-metal toxins (e.g., Cd, Hg); organic compounds, likewise, seem to be rare or absent. Although complete toxicology assessments require knowledge of how elements are combined into compounds (in addition to bulk-elemental assays), we can say that none of the minerals inferred from *VL* results or found in SNC meteorites presents a recognized toxic hazard. Indeed, the only significant issue surrounds interpretation of the unidentified trace-level reactants discovered by the *VL* biology experiments. Until the active agents are identified, however, we cannot assess their toxic potentials.

References: [1] Arvidson R. E., Gooding J. L., and Moore H. J. (1989) Rev. Geophys., 27, 39-60. [2] Aronson J. R. and Emslie A. G. (1975) J. Geophys. Res., 80, 4925-4931. [3] Singer R. B. (1982) J. Geophys. Res., 87, 10159-10168. [4] Gooding J. L., Wentworth S. J., and Zolensky M. E. (1988) Geochim. Cosmochim. Acta, 52, 909-915.

Table 1: Weight percent compositions of surface sediments (after B. C. Clark and others; summarized by [1])

	VL−1	VL−2	Uncertainty
SiO_2	44	43	± 6
TiO_2	0.62	0.54	± 0.25
Al_2O_3	7.3	n.d.	± 4
Fe_2O_3	17.5	17.3	−2 to +5
MgO	6	n.d.	−3 to +5
CaO	5.7	5.7	± 2
K_2O	≤ 0.5	≤ 0.5	± 0.5
SO_3	6.7	7.9	−2 to +6
Cl	0.8	0.4	−0.5 to +1.5

Notes: Expression as oxides is by convention; minerals and compounds not identified
n.d. = not determined because of instrument noise

Table 2: Possible dust-forming minerals found as grains in SNC meteorites (J. L. Gooding and collaborators)

	Shergottite EETA79001	Nakhla	Chassigny
$CaCO_3$	X	X	X
$CaSO_4 \cdot nH_2O$	X	X	X
$(Mg)_x(PO_4)_y \cdot nH_2O$	X		
$(Mg)_x(SO_4)_y \cdot nH_2O$		X	
NaCl		X	
S,Cl−aluminosilicate	X		
Smectite (?) $(Ca,K,Mg)_{0.2}(Fe,Mg)_2(Si,Al,Fe)_4O_{10}(OH)_2 \cdot nH_2O$		X	

WIND ABRASION ON MARS *R. Greeley, Department of Geology, Arizona State University, Tempe, AZ 85287-1404*

Aeolian activity was predicted for Mars from earth-based observations of changing surface patterns that were interpreted as dust storms. Mariner 9 images showed conclusive evidence for aeolian processes in the form of active dust storms and various aeolian landforms including dunes and yardangs. Windspeeds to initiate particle movement are an order of magnitude higher on Mars than on Earth because of the low atmospheric density on Mars. It was reasoned that saltating particles on Mars therefore would travel much faster than on Earth and would be effective agents of abrasion. This consideration, coupled with the frequent dust storms observed telescopically, led to predictions of extremely high rates of aeolian erosion (Sagan, 1973; Henry, 1975). Viking results, however, led to a reassessment of wind erosion on Mars. The Viking orbiters reveal surfaces that have small (~10 m) impact craters whose presence indicate surfaces that are millions or even hundreds of millions of years old but which have been little modified by erosion of any type (Arvidson et al., 1979). If the rates predicted prior to the Viking mission were correct, these craters should have been "erased" long ago.

In order to determine rates of abrasion by wind-blown particles, knowledge of three factors is required (Figure 1): (1) particle parameters such as numbers and velocities of windblown grains as functions of windspeeds at various heights above the surface, (2) the susceptibility to abrasion (S_a) of various rocks and minerals, and (3) wind frequencies and speeds. For estimates appropriate to Mars, data for the first two parameters can be determined through laboratory and wind tunnel experiments; data for the last factor are available directly from the Viking Lander (VL) meteorology experiments for the two landing sites.

Experiments (Greeley et al., 1982) have been conducted to collect information on the parameters required for Mars. Assuming an abundant supply of sand-sized particles, estimated rates range up to 2.1×10^{-2} cm of abrasion per year in the vicinity of Viking Lander 1. This rate is orders of magnitude too great to be in agreement with the inferred age of the surface based on models of impact crater flux. The discrepancy in the estimated rate of abrasion and the presumed old age of the surface cannot be explained easily by changes in climate or exhumation of ancient surfaces. The primary reason for the discrepancy appear to be related to the agents of abrasion. Either windblown grains are in very short supply, or the grains are ineffective as agents of abrasion. At least some sand-sized (~100 μm) grains appear to be present, as inferred from both lander and orbiter observations. High rates of abrasion occur for all experimental cases involving sands of quartz, basalt, or ash. However, previous studies have shown that sand is quickly comminuted to silt- and clay-sized grains in the martian aeolian regime. Experiments also show that these fine grains are electrostatically charged and bond together as sand-sized aggregates (Greeley, 1979). Laboratory simulations of wind abrasion involving aggregates show that at impact velocities capable of destroying sand, aggregates form a protective veneer on the target surface and can give rise to extremely low abrasion rates (Greeley et al., 1982).

It must be noted, however, that rates of abrasion at the scale of rocks centimeters to meters in size cannot be extrapolated to rates of erosion at the > kilometer-scale of landforms such as craters, and the rate of surface erosion determined by the preservation of impact craters may not be appropriate for consideration of abrasion of spacecraft. Moreover, the experiments outlined here emphasize the importance of the supply of sand-size material. Although such grains may be in short supply at the two Viking Landing sites, they may be abundant in other regions as evidenced by sand dunes.

References:

Arvidson, R., E. Guinness, and S. Lee, Differential aeolian redistribution rates on Mars, *Nature, 278*, 533-535, 1979.

Greeley, R., Silt-clay aggregates on Mars, *J. Geophys. Res., 84*, 6248-6254, 1979.

Greeley, R., R.N. Leach, S.H. Williams, B.R. White, J.B. Pollack, D.H. Krinsley, and J.R. Marshall, Rate of Wind Abrasion on Mars, *J. Geophys. Res., B12*, 10,009-10,024, 1982.

Henry, R.M., Saltation on Mars and expected lifetime of Viking 75 wind sensors, *NASA Tech. Note, D-8035*, 39 pp., 1975.

Sagan, C., Sandstorms and eolian erosion on Mars, *J. Geophys. Res., 78*, 4155-4161, 1973.

N91-27065

THE AEOLIAN WIND TUNNEL

J.D. Iversen, Department of Aerospace Engineering, Iowa State University, Ames, IA 50010

The aeolian wind tunnel is a special case of a larger subset of the wind tunnel family which is designed to simulate the atmospheric surface layer winds to small scale (a member of this larger subset is usually called an atmospheric boundary layer wind tunnel or environmental wind tunnel). The atmospheric boundary layer wind tunnel is designed to simulate, as closely as possible, the mean velocity and turbulence that occur naturally in the atmospheric boundary layer (defined as the lowest portion of the atmosphere, of the order of 500 m, in which the winds are most greatly affected by surface roughness and topography). The aeolian wind tunnel is used for two purposes: (1) to simulate the physics of the saltation process and (2) to model at small scale the erosional and depositional processes associated with topographic surface features.

A long test section for the environmental wind tunnel is desirable in order to achieve sufficient boundary layer depth, turbulence characteristics, and for the aeolian wind tunnel, equilibrium particle transport rate. Although the side-walls restrict lateral motion of the wind compared to the natural atmosphere, and the turbulent spectrum is "narrower" (i.e., the frequency of the maximum energy containing eddies is higher than for the natural atmosphere), that descrepancy is not as important for sand-sized particles (> 100 μm) as it is for modeling transport by suspension (diffusion of dust particles < 100 μm). Other important considerations for modeling saltation phenomena include minimum criteria for Reynolds number ($u_*^3/g\nu$, $U_\infty x/\nu$) and maximum criteria for Froude number (U_∞^2/gH, u_*^2/gH).

Minimum size requirements for the aeolian wind tunnel are based on the necessity for development of a thick turbulent boundary layer, for equilibrium of mass transport rate as a function of downwind distance, and for (small-scale modeling) the geometric scale ratio desired. The upper limit to wind tunnel size is determined by practicability, available space, and cost. Owen and Gillette (1985) have suggested a lower limit on wind tunnel height based on wind tunnel Froude number. Recent experimental data seem to confirm Owen's criterion of a maximum wind tunnel speed during saltation. The criterion is based on a maximum wind tunnel Froude number, i.e.,

$$\frac{U_\infty^2}{gH} \leq 20 \qquad (1)$$

where U_∞ is the wind tunnel free stream speed and H the test section height. For Froude numbers above that value, the shear stress, and thus mass transport rate, might not reach an equilibrium value in the wind tunnel. Cermak (1982) has suggested a minimum wind tunnel length criterion based on tunnel length Reynolds number to achieve a thick turbulent boundary layer. His criterion is

$$(2) \qquad L \geq 3.47\,\delta\,(\delta U_\infty/\nu)^{1/4}$$

where δ is the desired boundary layer thickness and ν is kinematic viscosity. The minimum test section length for a boundary layer depth of H/4 for the aeolian wind tunnel according to these criteria can be found by combining Eqns. (1) & (2):

$$(3) \qquad L \geq 0.89\,(H^{11}\,g/\nu^{2})^{1/8}$$

For purposes of investigating aeolian effects on the surfaces of Mars and Venus as well as on Earth, the aeolian wind tunnel continues to prove to be a useful tool for estimating wind speeds necessary to move small particles on the three planets as well as to determine the effects of topography on the evolution of aeolian features such as wind streaks and dune patterns.

N91-27066

MEASUREMENTS OF DUST ON MARS TO BE OBTAINED FROM UPCOMING MISSIONS. Bruce M. Jakosky, Laboratory for Atmospheric and Space Physics and Department of Geological Sciences, University of Colorado, Boulder, CO 80309-0392.

Measurements of dust on the Mars surface and in its atmosphere will be made from several upcoming missions. The best-defined missions are Mars Observer, the Soviet Mars 94 mission, and the Mars Environmental Survey (MESUR) mission. Following is a discussion of what measurements pertaining to airborne or surface dust will be made and what properties can be inferred from them. The payloads for the latter two missions are, of course, not yet determined or absolutely known. In all cases, only that information which pertains to dust is included; each mission contains additional instruments that provide no information on this topic. Following the discussion of individual instruments is a summary of the types of measurements and observations that will be made from the ensemble collection of instruments and missions, and a brief discussion of the types of measurements of dust which will not be made. This revised abstract contains the results of the group discussion from the workshop.

Observations of dust to be made from upcoming missions:

Mars Observer (MO):

Pressure Modulator Infrared Radiometer (PMIRR):

- Vertical profile of dust absorption coefficient
  - Column abundance, spatial and vertical distribution of dust amount in atmosphere
- Thermal emission from surface
  - Some information on surface structure
- Vertical profiles of temperature
  - Clues to dust-induced atmospheric dynamics

Thermal Emission Spectrometer (TES):

- Emission spectrum of dusty atmosphere
  - Particle-size distribution of airborne dust
  - Composition of airborne dust
- Vertical profile of emission spectrum of airborne dust
  - Vertical distribution of dust
  - Variations in composition or particle size with height
- Emission spectrum of surface
  - Surface structure (thermal inertia, block abundance, etc.)
  - Composition and mineralogy of dust on the surface

Gamma-Ray Spectrometer (GRS):

- Relative numbers of atoms at the surface
  - Surface composition, global variability of dust

Camera (MOC):

High-resolution images of the surface
Surface structure, block abundance, etc.
Clues to ongoing geomorphological processes pertaining to sand and dust
Moderate-resolution images of the surface
Temporal changes in surface albedo related to deposition or removal of dust from the surface
Low-resolution (daily) global images in two colors
Spatial information on dust distribution, with clues to the genesis of global and local dust storms

Laser Altimeter (MOLA):

Altitude of whatever reflects at 1.06 microns
Possible heights of discrete dust clouds or local dust storms

Radio Science (RS):

High-vertical-resolution atmospheric structure in polar regions
Clues to dust-induced atmospheric dynamics

Mars Environmental Survey (MESUR):

Atmospheric structure experiment:

Entry profile of temperature and winds in lower atmosphere
Clues to dust-induced atmospheric dynamics

Descent/surface imaging:

High-resolution images of surface
Surface structure, block abundance, etc.
Clues to ongoing geomorphological processes pertaining to sand and dust

Meteorology at surface:

Diurnal variation in atmospheric pressure
Clues to dust-induced atmospheric dynamics
Winds at surface
Clues to dust-induced atmospheric dynamics
Information on ability of wind to raise dust or to saltate sand

Atmospheric opacity at surface:

Atmospheric opacity of dust at surface
Atmospheric opacity of dust at surface

Surface composition experiment:

Elemental abundances at surface
Composition and mineralogy of surface

Differential thermal analysis experiment:
Volatile content of surface materials

Mars 94:

(Orbiter)

Overall mission
Diurnal variability at local times other than will be obtained from other missions, due to different orbit

TV camera:

High-resolution images of the surface (about 10 m/pixel, four-color, stereo)
Clues to ongoing geomorphological processes pertaining to sand and dust
Three-dimensional structure at scales larger than 10 m

Omega (Infrared Spectrometer):

Surface reflection spectra between 1 and 5 microns
Surface mineralogy

Fourier spectrometer:

Thermal emission spectra between 1.2 and 40 microns
Particle-size distribution of airborne dust
Composition of airborne dust
Surface structure (thermal inertia, blocks, etc.)
Composition and mineralogy of dust on the surface

Stellar occultation atmospheric spectrometer:

Vertical profiles of stellar radiance through the atmosphere
Vertical profiles of atmospheric dust absorption, and column opacity

Gamma-Ray Spectrometer:

Relative number of atoms at the surface
Surface composition, global variability of dust

Termoskan:

Broadband thermal emission from surface

Surface thermal inertia and spatial variability

Radar sounder (at multiple frequencies near 1 Mhz):

Electrical properties of surface (if ionosphere is absent)
Density of near-surface layer
Possible vertical structure of surface
Possible presence of liquid water

(Balloon)

Gondola

TV camera:

High-resolution images of the surface
Spatial variability of surface features and dust clouds

Meteorology package:

Structure of atmosphere within diurnal boundary layer
Clues to dust-induced atmospheric dynamics

Infrared Spectrometer:

Dust composition and mineralogy

Aerosol sensor:

Column dust opacity

Electromagnetic induction sounder:

Electrical properties of subsurface
Structure of subsurface at kilometer scale
Possible presence of liquid water

Snake

Gamma-ray Spectrometer:

Same as above

Accelerometers:

Structure and cohesion of surface at small scales

Ground-penetrating radar (approx. 1 m wavelength in ground)

Electrical properties of surface layer
Structure of top 100 m of regolith
Possible presence of liquid water

Rover

TV camera:

Images of the surface at high spatial resolution

Alpha-proton spectrometer:

Numbers of atoms in surface materials
Composition and mineralogy of surface

Reflection and fluorescence spectrometer:

Surface composition and mineralogy

Mossbauer spectrometer:

Surface mineralogy

Electrostatic instrument:

Electrostatic properties of dust/atmosphere

Penetrator

TV camera, viewing over 360 degrees:

Same as above

Gamma-ray Spectrometer:

Same as above

The following is a list of the types of information that will be obtained from the above instruments, sorted by type of information rather than by instrument or mission. The missions which will measure each piece of information are listed (MO = Mars Observer, M94 = Mars 94, MSR = MESUR; S indicates that some type of synoptic coverage will be obtained, and L indicates that information will be obtained only at discrete or small number of times/locations, where appropriate).

ATMOSPHERIC DUST

1. Vertical profiles of temperature and dust absorption through the atmosphere.
   MO/S, M94/S, MSR/L

2. Particle size distribution of airborne dust, within range of about 1 to 10 microns; less-detailed information on sizes down to about 0.1 micron.
   MO/S, M94/S

3. Some information on vertical profiles of particle size distribution.
   MO/S, M94/S

4. Some information on composition of dust and on vertical profiles of compositional variation.
   MO/S, M94/S

5. Spatial distribution of atmospheric dust clouds or storms.
   MO/S, M94/?

6. Column opacity of airborne dust, and spatial variations.
   MO/S, M94/S, MSR/L

7. Direct measure of winds/dynamical properties at some locations and times.
   MO/S, M94/S, MSR/L

SURFACE DUST

1. Information on sources and sinks of atmospheric dust.
   MO/S, M94/S

2. Elemental composition of surface materials.
   MO, M94, MSR/L

3. Mineralogy of surface materials.
   MO, M94

4. Thermal inertia, block abundance and size distribution.
   MO, M94, MSR/L

5. Geologic information at high spatial resolution over some fraction of the surface (and clues to ongoing geological processes).
   MO, M94, MSR/L

6. Some information on cohesion of the surface at a single location (from Mars 94 penetrator).
   M94/L

7. Some information on trafficability of surface at a single location (from Mars 94 rover).
   M94/L

8. Some information on thickness of dust deposits and structure of near-surface layer.
M94

9. Presence or absence of liquid water within regolith, at varying vertical scales.
M94

10. Some information on electrostatic properties of surface dust.
M94/?

The following list includes information that is pertinent to the properties or evolution of dust on the surface and in the atmosphere but which will not be obtained by any of these missions or instruments. Notice that some information could be obtained by instruments which could still find their way onto the payload of MESUR or Mars 94. Also listed is the type of instrument which could make the desired measurements, if possible and if known.

1. Actual particle size and shape distribution of dust in the atmosphere and on the ground (particle counters; sky brightness and polarization measurements; optical and electron microscopes).

2. Global information on cohesion of surface dust or fine materials and on trafficability of surface materials (could be obtained from a small number of landed packages, in conjunction with global remote-sensing observations).

3. Electrostatic properties of surface/airborne dust and atmospheric breakdown of electrical conductivity (in-situ (landed) DC voltmeter).

4. Chemical properties of surface dust (such as chemical reactivity, corrosiveness) (essentially same experiment as electrostatic properties).

5. Detailed information on incremental and net motion of surface and airborne dust over the course of a year (sounding board particle counter for movement of sand-sized grains; yardstick stuck into ground; observations over many years).

6. Direct measure of shear stress at surface (wind velocity at three heights above surface).

7. Direct measure of mineralogy (currently to be done possibly on one landed package) (XRD; Infrared spectrometer; cross-polarized optical microscope).

8. Toxicity (send a rabbit).

9. Dust-deposit thickness (cores; EM sounding; penetrator; seismometer).

N91-27067

ENGINEERING KNOWLEDGE REQUIREMENTS FOR SAND AND DUST ON MARS

D. I. Kaplan, Lunar & Mars Exploration Program Office, NASA/Johnson Space Center

The successful landing of human beings on Mars and the establishment of a permanent outpost there will require an understanding of the martian environment by the engineers. A key feature of the martian environment is the nearly ubiquitous presence of sand and dust.

The engineering community will be tasked to perform many critical functions at Mars. Each of these functions will certainly be influenced by the sand and dust in the environment. For example, safe landing (entry, descent, and touchdown) will require good visibility, knowledge of atmospheric density, and an aeroshell which will not be critically eroded. Habitat emplacement will require appropriate site selection, site preparation, actual emplacement of the habitat, and emplacement of radiation protection around the habitat. Surface operations will require surface mobility and mining (including the location of resources as well as excavation). The effects of sand and dust on equipment will be of great importance to many scientific and engineering functions.

The engineering teams will begin with the best understanding of sand and dust from the scientific community, and they will evaluate the sensitivities of their engineering designs and operations to that knowledge. In some areas, a broad range of possible sand and dust values will have little effect on outpost or vehicle designs. In other areas, knowledge which is lacking, or uncertainties which are high, may potentially have a huge influence on the designs and operations. For these latter cases, the mission planners of the Space Exploration Initiative (SEI) will need to evaluate the advantages of acquiring precise martian environmental data through the flights of robotic precursor missions.

The paper will focus on the process which the engineering community will undertake to determine the sensitivities of their designs to the current level of knowledge about Mars sand and dust. It will also describe the interaction of the engineering community with the SEI mission planners and management.

N91-27068

ELECTRICAL SYSTEM/ENVIRONMENT INTERACTIONS ON THE PLANET MARS

J.C. Kolecki, G.B. Hillard, and D.C. Ferguson, Space Environment Interactions Br., NASA Lewis Research Center, NASA 2100 Brookpark Road, Cleveland, OH 44135

The Martian environment is a diverse environment with which systems will interact in numerous ways. The following comments are preliminary thoughts on electrical system/environment interactions which might be of interest to system designers at all stages of system design.

Stationary surface sand and dust may be subject to electrical charging due to incident solar ultraviolet light which reaches the Martian surface at an intensity approximately equal to its value in Mars space. Additionally, sand and dust charging could also occur around electrically powered systems by induced dipole coupling effects with exposed high voltage surfaces. When such charging occurs, regardless of the mechanism involved, Coulombic forces result in the sand and dust being attracted and adhering to surfaces, thereby modifying surface thermal, optical, and dielectric properties. Stationary surfaces will acquire variable coatings of sand and dust which must be dealt with both in system design, and later, in situ on the Martian surface. Further, sand and dust transported on roving vehicles, and/or human explorers moving out of and into controlled volumes could pose a significant contamination problem.

Wind borne dust may also be subject to electrical charging due to triboelectric mechanisms. Differential settling of triboelectrically charged dust following major dust storms may result in significant charge seperation with concomitant electrical breakdowns between surfaces, or to the Martian ground or atmosphere. Additionally, the presence of variable levels of sand and dust in the Martian atmosphere may significantly modify atmospheric electrical properties as seen by systems on the Martian surface. As a gas, the 7 - 9 Torr surface atmosphere is ideal for Paschen electrical breakdown over mm to cm distances at a few hundred volts, and cm to m distances at a few kilovolts. Atmospheric dust will certainly modify the breakdown properties of the atmosphere, acting possibly to seed or suppress breakdown phenomena around high voltage surfaces depending on such factors as atmospheric dust concentration, dust surface adhesion (or lack thereof), and dust dielectric properties. Paschen breakdown phenomena have been observed on Earth in simulated Martian conditions, and are known to result in system power loss and electromagnetic noise. Transient and sustained electrical discharges in general may sputter erode surfaces and result in contamination due to transport and redeposition of material.

The question which is of most interest here is: What happens when you add a system to an environment and "shake well?" How does one characterize the resulting interaction and use that knowledge to produce optimal system designs? Some areas for consideration/development include:

1.) Identifying relevant physical mechanisms/equations
2.) Producing, and (where necessary) experimentally verifying mathematical models
3.) Understanding user needs and establishing appropriate user interfaces
4.) Establishing appropriate input/output formats
5.) Identifying/performing relevant laboratory/space tests and analyses
6.) Delivering user-friendly software with appropriate interfaces

The Space Environment Effects Branch has worked for almost two decades on the development of analysis tools and computer software for use in designing systems for the LEO and GEO plasma environments. This software includes NASCAP/LEO and NASCAP/GEO (NASCAP = NASA Charging Analysis Program), which model system-plasma interactions including spacecraft charging, arcs and transient phenomena, anomalous switching, spacecraft grounding effects, and numerous related issues. Other software packages (EPSAT, and SSF ENVIRONMENT WORKBENCH) are also under development which will provide frameworks into which specific environment and system models may inserted, and interactions predicted. The charter of the Space Environment Effects Branch is to develop and provide modeling and analysis tools for the interactions between given environments and given systems, and to conduct whatever experimental and/or flight activities are necessary to validate those tools. With the advent of the Space Exploration Initiative, it seems appropriate that interactions models be developed for the moon and Mars. These models will provide systems engineers with unique, user-friendly tools which will couple the environmental models currently under development with systems models either extant or yet to be developed, and to predict the interplay of the two from an electrical/plasma interactions point of view. This capability will enable the best possible use of the environmental models for the moon and Mars in the production of optimal system designs.

N91-27069

EFFECT OF PRESSURE ON ELECTROSTATIC PROCESSES ON MARS

R. N. LEACH, Arizona State University at NASA-Ames Research Center, Mail Stop 242-6, Moffett Field, Ca. 91035

Paschen's Law as illustrated by Paschen curves for various gases (Figure 1) shows that the minimum breakdown voltage for gases for breakdown distances of interest i.e. 1-1000 mm will be at or near the surface pressure on Mars. This means that the physics of many electrostatic processes will be markedly different on Mars than on Earth.

The primary effect will be that voltage potentials above 100 volts will most certainly be subject to breakdown in the martian atmosphere. The curves of Figure 1 are the minimums produced under ideal conditions with smooth, clean electrodes. Sharp electrodes, dusty atmosphere conditions or other anomalies will modify the breakdown voltage, usually causing lower breakdown voltages.

Paschen's curves for most common pure gases have been experimentrally determined. A very small amount of mixing of different gases radically changes the curve as shown in the curve for neon plus 0.1% argon compared to either neon or argon. Paschen's curve for the exact composition of gases for Mars has not been determined and thus the breakdown voltages are not known.

A second important effect is that the breakdown for most martian cases will be a glow discharge rather than a spark discharge. It would seem that simple measurements of breakdown manner and voltage should be included on a Mars lander vehicle

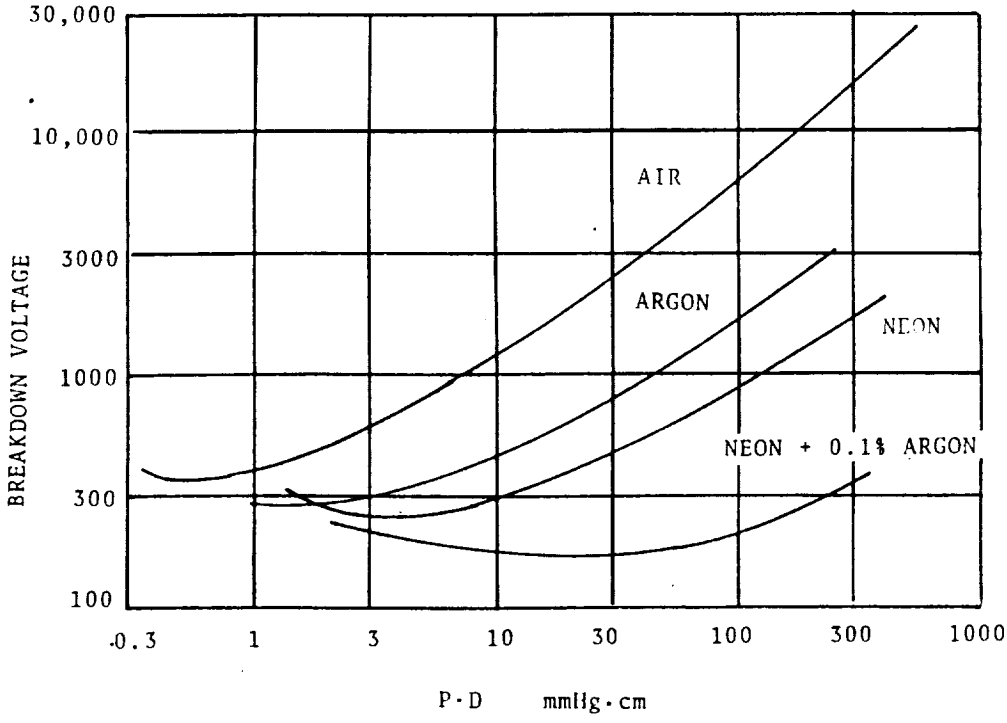

FIGURE 1 PASCHEN'S CURVES

N91-27070

SALTATION THRESHOLD DETECTION IN A WIND TUNNEL BY THE MEASUREMENT OF THE NET ELECTROSTATIC CHARGE

R.N. Leach, Arizona State University at NASA-Ames Research Center, Mail Stop 241-6, Moffett Field, CA 91035

MARSWIT (Mars Surface Wind Tunnel) is an open circuit wind tunnel used for aeolian studies and is located inside a large vacuum chamber allowing testing at martian surface atmosphere pressure (Greeley et al., 1977). Since direct access is not available to the tunnel during operation at low pressure a remote method of saltation detection is needed. The bed is observed by means of closed circuit video, but it is often difficult to determine the initiation of threshold. The measurement by means of an electrometer of the net electric charge produced by the saltating particles has provided a reliable means of saltation threshold detection.

Saltating particles become charged several ways, both in wind tunnels and in a natural environment. The most significant of these methods are tribo-charging and contact charging, which always occur. Fracture charging may also occur under the high velocities associated with particle transport on Mars or under simulated martian conditions.

The method of detection used in MARSWIT is by allowing the saltating particles to impinge on a planar conducting surface normal to the flow that is connected to ground through a Keithly Electrometer. The signal from the electrometer is connected to a strip chart recorder along with the analog signal from the pitot tube transducer that is used to determine the wind velocity in the tunnel. Thus a record of wind velocity and the initiation of particle saltation is conveniently displayed together.

While both positive and negative charges are produced during saltation this method measures only the net charge and thus may be either positive or negative depending upon the particles being tested, the size and size distribution of the test material and the wind velocity.

This has proved to be a very trustworthy and sensitive method of saltation threshold detection, being especially useful with the smaller sized particles which are the most difficult to observe visually.

References: Greeley, R. et al. 1977. NASA TM 78423, 2a p.

N91-27071

SALTATION THRESHOLD REDUCTION DUE TO THE ELECTROSTATIC AGGLOMERATION OF FINE PARTICLES

R.N. Leach and ***R. Greeley,*** Department of Geology, Arizona State University, Tempe, AZ 85287-1404

Particles between 80 and 110 microns in diameter are the most easily moved by the wind. As the particle size decreases below 60 microns they are increasingly more difficult to move by surface winds and a number of experiments have been performed in an attempt to reduce the required wind velocity. These include (1) the bombardment of a bed of fine particles by particles near the optimum size, the larger particles kicking the fine particles into the windstream where they are entrained and (2) the electrostatic agglomeration of fine particles into sizes more easily saltated.

Particles have been formed into large agglomerates (up to 700 microns in diameter) electrostatically in an erosion devise that moves the particles at high speed in a low pressure environment by means of a rapidly spinning paddle wheel. It has required relatively long times to form such agglomerates, 10 to 20 minutes. Once formed these agglomerates will last for months, and if physically broken apart will readily re-form. These long-lasting agglomerates are more easily moved by the wind than the fines from which they are formed, but these agglomerates have not yet been produced in a wind tunnel probably due to the short duration of particle interaction time in the wind tunnel. If another method of agglomeration is verified, such as their formation in the atmosphere after a dust storm, this may be a valid process for the entrainment of fines at low to moderate windspeeds.

What has been observed in the wind tunnel is that fine particles cling electrostatically to larger, more easily moved particles, and thus are carried along when optimum sized particles are moved by the wind. This process would enhance the number of fine particles, removed from a bed of fines by method (1) above, but would not necessarily cause such fine particles to be entrained into the atmosphere unless some mechanism is discovered to remove the fines from the larger particles. In fact, it may be causing a reduction of the number of fines entrained in the atmosphere as they are electrostatically captured by the impinging larger particles.

N91-27072

THE EFFECTS OF ATMOSPHERIC DUST ON OBSERVATIONS OF MARTIAN SURFACE ALBEDO; S.W. Lee and R.T. Clancy, Laboratory for Atmospheric and Space Physics, Univ. Colorado, Boulder, CO 80309

The Mariner 9 and Viking missions provided abundant evidence that aeolian processes are active over much of the surface of Mars [1; 2]. Past studies have demonstrated that variations in regional albedo and wind streak patterns are indicative of sediment transport through a region [3; 4], while thermal inertia data [derived from the Viking Infrared Thermal Mapper (IRTM) data set] are indicative of the degree of surface mantling by dust deposits [5; 6; 7; 8; 9]. The visual and thermal data are therefore diagnostic of whether net erosion or deposition of dust-storm fallout is taking place currently and whether such processes have been active in a region over the long term. These previous investigations, however, have not attempted to correct for the effects of atmospheric dust loading on observations of the martian surface, so quantitative studies of current sediment transport rates have included large errors due to uncertainty in the magnitude of the "atmospheric contamination".

We have developed a radiative transfer model which allows the effects of atmospheric dust loading and variable surface albedo to be investigated [see related abstract, 10]. This model incorporates atmospheric dust opacity, the single scattering albedo and particle phase function of atmospheric dust, the bidirectional reflectance of the surface, and variable lighting and viewing geometry.

The Cerberus albedo feature has been examined in detail using this technique. Previous studies have shown the Cerberus region to have a moderately time-variable albedo [4]. IRTM observations obtained at ten different times (spanning one full martian year) have been corrected for the contribution of atmospheric dust in the following manner:

- A "slice" across the IRTM visual brightness observations was taken for each time step. Values within this area were binned to 1° latitude, longitude resolution.
- The atmospheric opacity (τ) for each time was estimated from [11]. As the value of τ strongly influences the radiative transfer modelling results, spatial and temporal variability of τ was included to generate an error estimate.
- The radiative transfer model was applied, including dust and surface phase functions, viewing and lighting geometry of the actual observations, and the range of τ [10].
- Offsets were applied to the visual brightness observations to match the model results at each τ.
- The "true surface albedo" was determined by applying the radiative transfer model to the offset brightness values, assuming $\tau = 0$ and a fixed geometry (0° incidence, 30° emission). Repetition of this technique for each time step allows values of albedo for specific locations to be tracked as a function of time (Figure 1).

The initial results for Cerberus indicate the region darkens prior to the major 1977 dust storms, consistent with erosion of dust from the surface (possibly contributing to the increasing atmospheric dust load). There is some indication of regional brightening during the dust storms followed by a general darkening, consistent with enhanced dust deposition during the storms followed by erosion of the added dust. There is only minor variability during the second year, consistent with little regional dust transport during that period.

The results of this study indicate that atmospheric dust loading has a significant effect on observations of surface albedo, amounting to albedo corrections of as much as several tens of percent. This correction is not constant or linear, but depends upon surface albedo, viewing and lighting geometry, the dust and surface phase functions, and the atmospheric opacity. It is clear that the quantitative study of surface albedo, especially where small variations in observed albedo are important (such as photometric analyses), needs to account for the effects of atmospheric dust loading. Our future work will expand this study to other regional albedo features on Mars.

This research was supported under NASA Planetary Geology grant NAGW 1378.

REFERENCES: [1] Veverka, J., P. Thomas, and R. Greeley (1977). A study of variable features on Mars during the Viking primary mission. *J. Geophys. Res. 82*, 4167-4187. [2] Thomas, P., J. Veverka, S. Lee, and A. Bloom (1981). Classification of wind streaks on Mars. *Icarus 45*, 124-153. [3] Lee, S.W., P.C. Thomas, and J. Veverka (1982). Wind streaks in Tharsis and Elysium: Implications for sediment transport by slope winds. *J.Geophys. Res. 87*, 10025-10042. [4] Lee, S.W. (1986). Regional sources and sinks of dust on Mars: Viking observations of Cerberus, Solis Planum, and Syrtis Major (abstract), In *Symposium on Mars: Evolution of its Climate and Atmosphere* (V. Baker et al., eds.), pp. 71-72, LPI Tech. Rpt. 87-01, Lunar and Planetary Institute, Houston. [5] Kieffer, H.H., T.Z. Martin, A.R. Peterfreund, B.M. Jakosky, E.D. Miner and F.D. Palluconi (1977). Thermal and albedo mapping of Mars during the Viking primary mission. *J. Geophys. Res. 82*, 4249-4295. [6] Christensen, P.R. (1982). Martian dust mantling and surface composition: Interpretation of thermophysical properties. *J. Geophys. Res. 87*, 9985-9998. [7] Christensen, P.R. (1986). Regional dust deposits on Mars: Physical properties, age, and history. *J. Geophys. Res. 91*, 3533-3545. [8] Christensen, P.R. (1986). The distribution of rocks on Mars. *Icarus 68*, 217-238. [9] Jakosky, B.M. (1986). On the thermal properties of martian fines. *Icarus 66*, 117-124. [10] Clancy, R.T., S.W. Lee, and D.O. Muhleman (1991). Recent studies of the optical properties of dust and cloud particles in the Mars atmosphere, and the interannual frequency of global dust storms, this volume. [11] Martin, T.Z. (1986). Thermal infrared opacity of the Mars atmosphere. *Icarus 66*, 2-21.

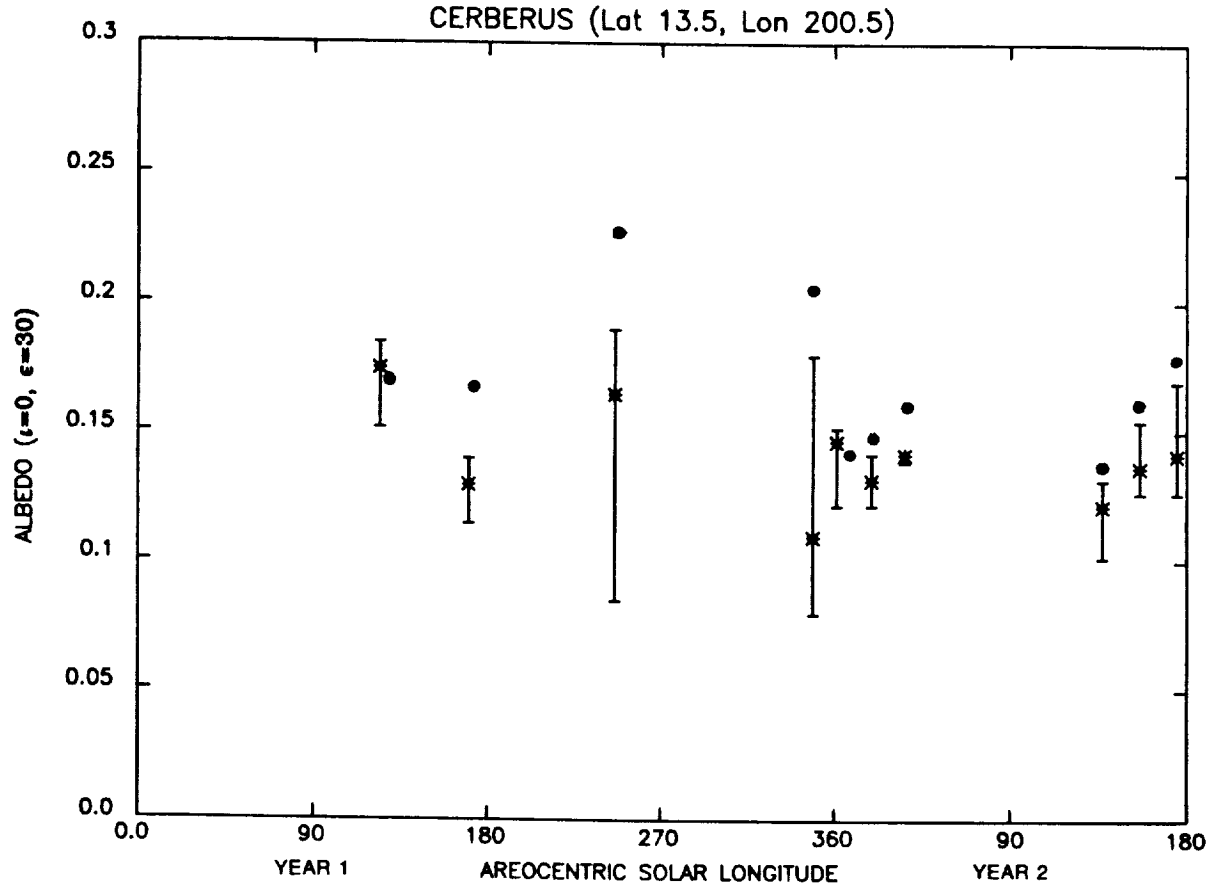

Figure 1: Temporal behavior of a dark area in Cerberus. "True surface albedos" are denoted by asterisks; error bars indicate uncertainty in τ. Uncorrected albedos are denoted by dots.

MARTIAN SURFACE MATERIALS

H. J. Moore, U.S. Geol. Survey, Menlo Park, CA, 94025

Our knowledge of the physical properties of the surface materials on Mars is very limited. 1. No experiments aboard the Viking Landers were designed to measure physical properties. 2. Orbital and Earth-based remote sensing observations have measurement uncertainties, model dependent interpretations, and different sensitivity scales and depths; large areas are sampled so that the physical properties of a number of components are integrated. 3. Some materials have not been properly sampled or not sampled at all. 4. Relevant laboratory data are incomplete. 5. Natural materials have variable physical properties that may not be separable with the available data. Despite these shortcomings, a semiquantitative appreciation for the physical properties of the surface materials and their global variations can be gained from the lander and remote sensing observations.

Analyses of Lander data yield estimates of the mechanical properties of the soillike surface materials [1,2] and "best guess" estimates can be made for the remote sensing signatures of the soillike materials at the landing sites [2,3]. Two soillike materials (blocky and crusty to cloddy) at the landing sites appear to be strong and compatible with natural soils, but the third (drift) presents a problem because it appears to be weak and unlike most natural soils. Footpad 3 of Lander 1 penetrated blocky material a few centimeters upon landing at about 2.4 m/s but footpad 2 penetrated 16.5 cm into drift material. It is unclear whether drift material, a strong substrate of blocky material, or buried rocks arrested the penetration of footpad 2 [2]. The friction angle for drift material (18±2.4°), estimated from the limits of surface deformation in front the sampler for trenches in drift material [1,2], is compatible with lunar regolith simulants [4] that have bulk densities about 800-900 kg/m^3, but the estimated cohesions (1.6±1.2 kPa; range: 0-3.7) are typically much larger. It is possible that the friction angle has been underestimated [5] and the cohesions overestimated. Smaller cohesions would be consistent with the lumpy appearance of the materials in the tailings of trenches, natural slope failures, and the stabilities of trench walls in trenches of drift material [2]. The friction angles and cohesions of the lunar regolith simulants are direct functions of the bulk densities [4]. If drift material is like the lunar regolith simulant, a friction angle about 27°, a cohesion about 40 Pa, and a bulk density about 1100 kg/m^3 is possible. This bulk density is the same as that of disturbed drift material [6]. Friction angles and cohesions between the extremes are possible, but drift material remains relatively weak.

Drift material is fine grained [7] and powderlike [2]; it has a low bulk density. Thus, the thermal inertia should be low and range from 1 to 3 X 10^{-3} cgs units [8,9,10,2,3]. This range of thermal inertias is comparable to those reported from orbital observations for vast regions on Mars such as Tharsis [11,12]. Powders and very porous rocks with bulk densities that range from 800 to 1100 kg/m^3 should have relative dielectric constants that range from about 1.8 to 2.2 [13]. Normal reflectivities of quasi-specular radar echoes from the Tharsis region [14,15,16] suggest relative dielectric constants in this range. Color reflectances vary but they are like telescopic bright areas [17,18]. Thus, significant thicknesses of powderlike surface materials with physical properties similar to drift material are present on Mars and probably pervasive in the Tharsis region.

Crusty to cloddy material is fine grained [19], reasonably strong, and moderately dense (1400 kg/m^3) with estimated friction angles of 34.5±4.7° [1,2]. These friction angles are compatible with those of natural dry loess [20] and lunar regolith simulants [4] with moderate bulk densities. Cohesions (1.1±0.8 kPa; range: 0-3.2) are less than those of the loess, but larger than those of the lunar regolith simulants. Upon disruption, crusty to cloddy material breaks into thin crusts and prismatic clods, suggesting that the material is cemented. The effect of cementation on thermal inertias is not understood, but cementation should increase thermal inertias [21]. The thermal inertia has been estimated to be about 5.6 to 6.3 X 10^{-3} cgs units [2,3], using Orbiter thermal [22] and Lander data and theory [23]. These inertias are near the principal modal values for the bulk and fine component thermal inertias determined from Orbiter thermal data [11,12]. The relative dielectric constant of this material should be about 2.8 [3] and comparable to the 3.0 inferred from average normal reflectivities of quasi-specular radar echoes from Mars [14]. Although color reflectances vary, they resemble telescopic bright regions [17,18]. Thus, it appears likely that soillike materials similar to crusty to cloddy material are typical for Mars.

Blocky material is also strong, cemented, and possibly moderately dense. Upon disruption, it forms centimeter-size clods that are more coherent than those of crusty to cloddy material [2]. The friction angles (30.8±2.4°) are comparable to natural dry loess [20]. Cohesions (5.1±2.7 kPa; range: 2.2-10.6) are typically smaller than those of the loess (> 10 kPa) but larger than those of the lunar regolith simulants (40-100 Pa) for the same friction angles. The thermal inertia has been estimated to be about 8.2 to 9.3 X 10^{-3} cgs units [2,3]. The relative dielectric constant should be about 3.3 [3]. Color reflectances are similar to drift material [17]. Thus, it appears likely that soillike materials similar to blocky material are common on Mars.

Surface and near-surface rocks are probably abundant. About 19% of the surface at the Lander 2 site is covered by rocks (> 0.04 m) [3]. Assuming that entire rock populations have effective thermal inertias of 30 X 10^{-3} cgs units, 20±10% and 15±5% of the Lander 2 and 1 sites, respectively, are covered by rocks; the modal coverage is 6% and the range from 1 to 30% [24]. 12.6-cm depolarized echoes imply considerable variations in areal coverage by wavelength-size (0.08-0.76 m) rocks and similar roughness elements at and near the surface [13,14,25]; globally, the smallest area covered by rocks is about 3%, the greatest about 76%, and commonly about 4% [25]. Rocks on the surface were never sampled by the landers [2], but they should be like terrestrial rocks with friction angles about 60°, cohesions measuring in MPa, thermal inertias ranging from 30 to 60 X 10^{-3} cgs units (depending chiefly on their size), and relative dielectric constants ranging from about 8 to 9 [13]. Color reflectances of rock surfaces vary: some resemble telescopic dark regions and unoxidized basaltic andesite coated with about 30 μm of palagonite, others telescopic bright regions and palagonite, and still others local "soils" [17,18]. Rare rock fragments resemble mafic rocks [26].

The physical properties of martian surface materials vary with location. Successful interpretations of these properties will require the combined use of as much available information as possible such as lander, thermal inertia, radar, albedo-color, and, especially, high-resolution imaging data on Mars.

REFERENCES: [1] Moore, H.J., et al., 1982, A summary of Viking sample-trench analyses for angles of internal friction and cohesions: J. Geophys. Res., v. 87, p. 10,043-10,050. [2] Moore, H.J., et al., 1987, Physical properties of the surface materials of the Viking landing sites on Mars: U.S.G.S. Prof. Paper 1389, 222 p., 2 plates. [3] Moore, H.J., and Jakosky, B.M., Viking landing sites, remote sensing observations, and physical properties of martian surface materials: submitted to Icarus. [4] Mitchell, J.K., et al., 1972, Mechanical properties of lunar soil: Density, porosity, cohesion, and angle of internal friction: Proc. 3rd Lunar Sci. Conf., Sup. 3, Geochim. et Cosmochim. Acta, v. 3, p. 3235-3253. [5] Scott, R.F., 1982, Soil mechanics tests with Viking Surface Sampler: Unpublished report, Div. Engr. and Appl. Sci., Soil Mech. Lab., Calif. Inst. of Technology, Pasadena, CA, 58 p. [6] Clark, B.C. III, et al., 1977, The Viking X-ray fluorescence experiment: Analytical methods and early results: J. Geophys. Res., v. 82, p. 4577-4594. [7] Ballou, E.V., et al., 1978, Chemical interpretation of Viking Lander 1 life detection experiment: Nature, v. 271, no. 5646, p. 644-645. [8] Wechsler, A.E., and Glaser, P.E., 1965, Pressure effects on postulated lunar materials: Icarus, v. 4, p. 335-352. [9] Wechsler, A.E., et al., 1972, Thermal properties of granulated materials: Astronautics and Aeronautics, v. 28, p. 215-241. [10] Fountain, J.A., and West, E.A., 1970, Thermal conductivity of particulate basalt as a function of density in simulated lunar and martian environments: J. Geophys. Res., v. 75, p. 4063-4069. [11] Palluconi, F.D., and Kieffer, H.H., 1981, Thermal inertia mapping of Mars from 60° S to 60° N: Icarus, v. 45, p. 415-426. [12] Christensen, P.R., 1986, Regional dust deposits on Mars: Physical properties, age and history: J. Geophys. Res., v. 91, p. 3533-3545. [13] Campbell, M.J. and Ulrichs, J., 1969, Electrical properties of rocks and their significance for lunar radar observations: J. Geophys. Res., v. 74, p. 5867-5881. [14] Downs, G.S., et al., 1975, Radar measurements of martian topography and surface properties: The 1971 and 1973 oppositions: Icarus, v. 26, p. 273-312. [15] Harmon, J.K., and Ostro, S.J., 1985, Mars: Dual-polarization radar observations with extended coverage: Icarus, v. 62, p. 110-128. [16] Harmon, J.K., et al., 1982, Dual-polarization radar observations of Mars: Tharsis and environs: Icarus, v. 52, p. 171-187. [17] Guinness, E.A., et al., 1987, On the spectral reflectance properties of materials exposed at the Viking landing sites: J. Geophys. Res., v. 92, p. E575-E587. [18] Arvidson, R.E., et al., 1988, The martian surface as imaged, sampled, and analyzed by the Viking Landers: submitted to Revs. Geophys., 48 p., 14 figs. [19] Oyama, V.I., and Berdahl, B.J., 1977, The Viking Gas Exchange Experiment results from Chryse and Utopia surface samples: J. Geophys. Res., v. 82, p. 4669-4676. [20] Gibbs, H.J., et al., 1961, Shear strength of cohesive soils: A.S.C.E. Res. Conf. (6/60), Boulder, CO, p. 33-162. [21] Jakosky, B.M. and Christensen, P.R., 1986, Global duricrust on Mars: Analysis of remote-sensing data: J. Geophys. Res., v. 91, p. 3547-3559. [22] Kieffer, H.H., 1976, Soil and surface temperatures at the Viking landing sites: Science, v. 194, no. 4271, p. 1344-1346. [23] Kieffer, H.H., et al., 1977, Thermal and albedo mapping of Mars during the Viking Primary Mission: J. Geophys. Res., v. 82, p. 4249-4291. [24] Christensen, P.R., 1986, The spatial distribution of rocks on Mars: Icarus, v. 68, p. 217-238. [25] Thompson, T.W. and Moore, H.J., 1989, A model for depolarized radar echoes from Mars: Proc. 19th Lunar and Planet. Sci. Conf., in press. [26] Dale-Bannister, M.A., et al., 1988, On the presence of unweathered lithic fragments in Viking Lander 1 soil: Abstracts Lunar and Planet. Sci. XIX, p. 239-240.

MAGNETIC AND ELECTRICAL PROPERTIES OF MARTIAN PARTICLES

G. R. Olhoeft, U.S. Geological Survey, POB 25046 DFC MS964, Denver, CO 80225-0046

The only determinations of the magnetic properties of Martian materials come from experiments on the two Viking landers (Hargraves et al., 1977, 1979). The results suggest Martian soil containing 1 to 10% of a highly magnetic phase. Though the magnetic phase mineral has not been conclusively identified, the predominate interpretation is that the magnetic phase is probably maghemite (Hargraves et al., 1977, 1979; Moskowitz and Hargraves, 1982; Bell et al., 1990; Coey et al., 1990, Morris et al., 1990).

The electrical properties of the surface of Mars have only been measured remotely by observations with earth based radar (selected references: Tyler et al., 1976; Simpson et al., 1978; Pettengill, 1978; Mouginis-Mark et al., 1980; Roth et al., 1985; Harmon, 1989; Moore et al., 1987; Moore and Jakosky, 1989; Thompson, 1989), microwave radiometry (Cuzzi and Muhleman, 1972; Epstein et al., 1983; Kuz'min and Losovskii, 1984), and inference from radio-occultation of Mars orbiting spacecraft (Tang et al., 1977; Lindal et al., 1979; Simpson et al., 1981, 1984). Such determinations are consistent with the electrical properties of lunar materials (Olhoeft, 1990) and of dry or frozen terrestrial silicates (Olhoeft and Strangway, 1974; Olhoeft, 1978). Such materials have relative dielectric permittivity that is given by $k' = 1.93^{d}$, where d is the dry bulk density in g/cm^3 (Olhoeft and Strangway, 1975), and the permittivity is independent of frequency. Beyond this, little is known for certain -- no direct measurements of electrical properties on Martian materials have been performed.

The volume electrical conductivity of such materials should be in the range of excellent insulators, roughly 10^{-9} to 10^{-14} Mhos/m. Such low electrical conductivity means the particles will have very low electromagnetic losses, with the principle attenuation due to surface and volume scattering mechanisms -- this means radiowaves will penetrate through Martian dust and soil for great distances. However, in the absence of water, such highly insulating surface materials will also result in problems for the grounding of electrical power systems and the creation of radio antenna ground planes for communication and navigation.

Further, such highly insulating particles may exhibit high surface electrostating charging and/or photoconduction effects as observed in lunar samples (Alvarez, 1975). The Apollo astronauts reported and drew pictures of "streamers" and corona/zodiacal light extending several kilometers above the lunar surface while approaching orbital sunrise. These are best explained as electrostatic levitation of soil particles (see further discussion and references in Olhoeft, 1990). The Apollo 17 LEAM (Lunar Ejector and Meteorites) experiment (Berg et al., 1973) found increased particle counts during passage of the terminator and:

"...all of the events recorded by the sensors during the terminator passages are essentially surface microparticles carrying a high electrostatic charge." "The particle event rate increases whenever the terminator passes over the instrument. This increase starts some 40 hours before sunrise and ends about 30 hours after it." (Rhee et al., 1977).

As the electrical conductivity is lowest during lunar night, the soil will have the highest electrostatic chargeability at night. It is possible that night-time activities which disturb the soil, will create dust that will thickly coat surfaces during the night. Upon sunrise, the resultant photo-induced increase in electrical conductivity will cause most of the coatings to discharge and slough off, leaving only a thin residual coating behind. During night, the low conductivity of the soil will also create significant electrical charging hazards between mobile objects on the surface -- producing the well known winter-time "spark" electrical discharge when the charged objects meet.

Similar electrostatic charging and coating effects may be found on the surface of Mars, though no experiments have been performed or are planned to look for such effects. These effects may be exacerbated by wind blown particle movement (which fosters charge separation and accumulation, resulting in lightning discharges during terrestrial desert sandstorms) or mitigated by the presence of water (Carr, 1986; Squyres, 1989) and millibar atmospheric pressure (which tends to produce electrostatic glow discharge instead of spark discharge). The effects of electrostatic charging and discharge on electronic equipment may also be a problem,

and are determined by the type of metal being charged, atmospheric pressure and composition, aerosol dust type and composition, incident radiation fields, and frequency. Some general reading on the effects of electrostatic charging and electrical properties of dust may be found in: Cox and Pearce, 1948; Brown, 1966; Whitby and Liu, 1966; Withers, 1979; John, 1980; Kunhardt and Luessen, 1983; Yeh et al., 1983).

The electrical properties of individual sand and dust particles will be dominantly those of silicate insulators. However, surface coatings on particles are possible where the activity of water has caused chemical alteration (such as clay or zeolite mineralization), desiccation (leaving behind salt), or frost. Little is known about the occurrence of such coatings, their electrical properties, or how they might modify the electrical properties of the particle substrate. In the absence of photoconductive effects, small quantities of moisture could dramatically alter the electrical behavior of Martian soil particles.

Alvarez, R., 1975, Lunar and terrestrial sample photoconductivity: Proc. Lunar Sci. Conf. 6th, p. 3187-3197.

Bell III, J. F., McCord, T. B. and Owensby, P. D., 1990, Observational evidence of crystalline iron oxides on Mars: JGR, v. 95, p.14,447-14,461.

Berg, O. E., Richardson, F. F., and Burton, H., 1973, Lunar ejecta and meteorites experiments, Apollo 17 Prelim. Sci. Report, NASA SP-330, chapter 16.

Brown, S. C., 1966, Introduction to electrical discharges in gases: NY, John Wiley & Sons, 286p.

Carr, M. H., 1986, Mars -- a water-rich planet?: Icarus, v. 68, p. 187-216.

Coey, J. M. D., Morup, S., Madsen, M. B. and Knudsen, J. M., 1990, Titanomaghemite in magnetic soils on Earth and Mars: JGR, v. 95, p. 14,423-14,425.

Cox, E. G. and Pearce, A. G., 1948, The ignition of dust clouds by electrostatic discharge: in Dust in Industry, Conf. at Leeds, England, 28-30 Sept 1948, Soc. of Chem. Industry, p. 113-121.

Cuzzi, J. N. and Muhleman, D. O., 1972, The microwave spectrum and nature of the subsurface of Mars: Icarus, v. 17, p. 548-560.

Epstein, E. E., Andrew, B. H., Briggs, F. H., Jakosky, B. M. and Palluconi, F. D., 1983, Mars, subsurface properties from observed longitudinal variation of the 3.5-mm brightness temperature: Icarus, v. 56, p. 465-475.

Hargraves, R. B., Collinson, D. W., Arvidson, R. E. and Spitzer, C. R., 1977, Viking magnetic properties experiment: primary mission results: JGR, v. 82, p. 4547-4558.

Hargraves, R. B., Collinson, D. W., Arvidson, R. E. and Cates, P. M., 1979, Viking magnetic properties experiment: extended mission results: JGR, v. 84, p. 8379-8384.

Harmon, J. K., 1989, Comparison of Mars radar scattering measurements at widely separated subradar latitudes: in Lunar and planetary science XX, LPI, p. 371-372.

John, W., 1980, Particle charge effects: in Generation of aerosols and facilities for exposure experiments, K. Willeke, ed., Ann Arbor, MI, Ann Arbor Science, p. 141-152.

Kunhardt, E. E. and Luessen, L. H., eds., 1983, Electrical breakdown and discharges in gases: Proceedings of a NATO Advanced Study Institute, Les Arcs, France, June 28 - July 10, 1981, NY, Plenum Press, 2 vols.

Kuz'min, S. O. and Losovskii, B. Y., 1984, Radiometric inhomogeneity of Mars at millimeter radio wavelengths: Solar System Res., 17, p. 119-124.

Lindal, G. F., Hotz, H. B., Sweetnam, D. N., Shippony, Z., Brenkle, J. P., Hartsell, G. V., Spear, R. T. and Michael, W. H., Jr., 1979, Viking radio occultation measurements of the atmosphere and topography of Mars, data acquired during 1 Martian year of tracking: JGR, v. 84, p. 8443-8456.

Moore, H. J., Hutton, R. E., Clow, G. D. and Spitzer, C. R., 1987, Physical properties of the surface materials at the Viking landing sites on Mars, USGS Prof. Paper 1389, 222p.

Moore, H. J. and Jakosky, B. M., 1989, Viking landing sites, remote sensing observations, and physical properties of Martian surface materials: Icarus, v. 81, p. 164-184.

Morris, R. V., Gooding, J. L., Lauer Jr., H. V. and Singer, R. B., 1990, Origins of Marslike spectral and magnetic properties of a Hawaiian palagonitic soil: JGR, v. 95, p. 14,427-14,434.

Moskowitz, B. M. and Hargraves, R. B., 1982, Magnetic changes accompanying the thermal decomposition of nontronite (in air) and its relevance to Martian mineralogy: JGR, v. 87, p. 10,115-10,128.

Mouginis-Mark, P. J., Zisk, S. H. and Downs, G. S., 1980, Characterization of martian surface materials from Earth-based radar--the Memnonia Fossae region: Proc. Lunar Planet. Sci. Conf. 11th, p. 823-838.

Olhoeft, G. R., 1978, The electrical properties of permafrost: in Prof. of the Third Int. Conf. on Permafrost, v. 1, Ottawa, Nat. Res. Council, p. 127-131.

Olhoeft, G. R., 1990, Electrical and electromagnetic properties: in Lunar Handbook, G. Heiken and D. Vaniman, eds., Cambridge Univ. Press.

Olhoeft, G. R. and Strangway, D. W., 1974, Electrical properties of the surface layers of Mars: GRL, v. 1, p. 141-143.

Olhoeft, G. R. and Strangway, D. W., 1975, Dielectric properties of the first 100 meters of the moon: EPSL, v. 24, p. 394-404.

Pettengill, G. H., 1978, Physical properties of the planets and satellites from radar observations: Ann. Rev. Astron. Astrophys., v. 17, p. 265-292.

Rhee, J. W., Berg, O. E., and Wolf, H., 1977, Electrostatic dust transport and Apollo 17 LEAM experiment, COSPAR Space Research, v.XVII, NY, Pergamon, p.627-629.

Roth, L. E., Saunders, R. S. and Schubert, G., 1985, Radar and the detection of liquid water on Mars: in Workshop on water on Mars, S. Clifford, ed., LPI Tech. Rep. 85-03, p. 71-73.

Simpson, R. A., Tyler, G. A. and Campbell, D. B., 1978, Arecibo radar observations of Martian surface characteristics in the northern hemisphere: Icarus, v. 36, p. 153-173.

Simpson, R. A., Tyler, G. A. and Campbell, D. B., 1978, Arecibo radar observations of Martian surface characteristics near the equator: Icarus, v. 33, p. 102-115.

Simpson, R. A., Tyler, G. L. and Schaber, G. G., 1984, Viking bistatic radar experiment, summary of results in near-equatorial regions: JGR, v. 89, p. 10385-10404.

Simpson, R. A. and Tyler, G. L., 1981, Viking bi-static radar experiment: summary of first-order results emphasizing north polar data, Icarus, 46, p. 361-389.

Squyres, S. W., 1989, Urey prize lecture: Water on Mars: Icarus, v. 79, p. 229-288.

Tang, C. H., Boak III, T. I. S. and Grossi, M. D., 1977, Bistatic radar measurements of electrical properties of the Martian surface: JGR, v. 82, p. 4305-4315.

Thompson, T. W., 1989, Goldstone radar observations of Mars: the 1986 opposition: in Lunar and planetary science XX, LPI, p. 1119-1120.

Tyler, G. L., Campbell, D. B., Downs, G. S., Green, R. R. and Moore, H. J., 1976, Radar characteristics of Viking 1 landing sites: Science, v. 193, p. 812-815.

Whitby, K. T. and Liu, B. Y. H., 1966, The electrical behavior of aerosols: in Aerosol science, ch.III, C. N. Davies, ed., NY, Academic Press, p. 65ff.

Withers, R. S., 1979, Transport of charged aerosols: NY, Garland publ., 444p.

Yeh, H.-C., Cheng, Y.-S. and Kanapilly, G. M., 1983, Use of the electrical aerosol analyzer at reduced pressure: in Aerosols in the mining and industrial work environments, v. 3, V. A. Marple and B. Y. H. Liu, eds., Ann Arbor, MI, Ann Arbor Science, p. 1117-1133.

N91-27075

REFLECTANCE SPECTROSCOPY OF PALAGONITE AND IRON-RICH MONTMORILLONITE CLAY MIXTURES: IMPLICATIONS FOR THE SURFACE COMPOSITION OF MARS

J.B. Orenberg and J.Handy, San Francisco State University, San Francisco, CA. 94132

Because of the power of remote sensing reflectance spectroscopy in determining mineralogy, it has been used as the major method of identifying possible mineral analogs of the martian surface. A summary of proposed martian surface compositions from reflectance spectroscopy before 1979 was presented by Singer et al. (1979, 1985). Since that time, iron-rich montmorillonite clay (Banin and Rishpon,1979; Banin et al., 1988), nanocrystalline or nanophase hematite (Morris et al.,1989), and palagonite (Evans and Adams, 1979; Allen et al., 1981; and Singer, 1982) have been suggested as Mars soil analog materials.

Palagonite in petrological terms is best described, perhaps, as an amorphous, hydrated, ferric iron, silica gel. Montmorillonite is a member of the smectite clay group and its structure is characterized by an octahedral sheet in coordination with two tetrahedral sheets in which oxygen atoms are shared. The crystallinity of montmorillonite is well defined in contrast to palagonite where it is considered amorphous or poorly crystalline at best.

Because of the absence of the diagnostic, strong 2.2 μm reflectance band characteristic of clays in the near infrared (NIR) spectrum of Mars and palagonite, and based upon a consideration of wide wavelength coverage (0.3-50 μm), Roush et al. (1989) concluded that palagonite is a more likely Mars surface analog. In spite of the spectral agreement of palagonite and the Mars reflectance spectrum in the 2.2 μm region, palagonite shows poor correspondence with the results of the Viking LR experiment (Banin et al., 1983, 1988). In contrast, iron-rich montmorillonite clays show relatively good agreement with the results of the Viking LR experiment (Banin et al., 1979, 1983, 1988).

This spectral study was undertaken to evaluate the spectral properties of mixtures of palagonite and Mars analog iron-rich montmorillonite clay (16-18 wt % Fe as Fe_2O_3) as a Mars surface mineralogical model. Mixtures of minerals as Mars surface analog materials have been studied before (Singer, 1982; Singer et al., 1985), but the mixtures were restricted to crystalline clays and iron oxides

Reflectance spectra from 0.3 to 2.5 μm were recorded on a Perkin Elmer Lambda 9 spectrophotometer (Norwalk, CT) using a Labsphere DRTA-9A Diffuse Reflectance and Transmittance Accessory (North Sutton, NH). Reflectance data presented below thus represent hemispherical reflectance. The spectral bandpass was set between 1/5 and 1/10 of the widths at half height of the spectral features of interest by setting the slits to 2.0 nm in the UV/VIS. This allowed for a constant spectral resolution (±10%) in the UV/VIS. In the NIR , an automatic slit program was used to maintain a constant energy level during spectral scanning (120 nm/min).

Mixtures (% by wt) of palagonite with the iron-rich Mars analog montmorillonite (15.8 ± 0.8 wt % Fe as Fe_2O_3 - a full Mars iron analog) are shown in the figures. In the very important 2.2 μm region, the band due to clay lattice structure becomes noticeable in mixtures at the 10 - 20 wt % Fe-montmorillonite level. In order to evaluate this observation more quantitatively, a rigorous band depth analysis was carried out (Clark and Roush, 1984). The results indicated that band depth at 2.2 μm is insensitive to the presence of up to 15 wt % Fe-montmorillonte. Above these concentrations, there is an increase in band depth with increasing wt % Fe-montmorillonite (decreasing palagonite) which is attributable to the 2.20 μm absorption feature characteristic of smectite clays. If one accepts the premise that palagonite is a

"good" spectral analog of the Mars surface material, up to 15 wt % of Fe-montmorillonite can be present on the surface of Mars and remain undetected. In spite of the fact that the most recent telescopic observations of Mars do not show evidence of a 2.20 μm band (Clark et al., 1990), the absence of the 2.20 μm band cannot be used to eliminate less than 15 wt % iron enriched montmorillonite. The conclusion follows that a Mars analog, iron rich, montmorillonite clay can be present on the surface of Mars as a major component (up to 15wt %) of the Mars soil even if the 2.20 μm band is absent from remotely sensed spectra.

References:[1]Singer, R.B., McCord, T.B., Clark, R.N., Adams, J.B., and Huguenin, R.L. 1979. J. Geophys Res., 84, 8415-8426;[2]Singer, R.B. 1982. J. Geophys. Res., 87, 10159-10168;[3]Banin, A and Rishpon, J. 1979. Life Sci. and Space Res. XVII, 59-64.;[4]Banin, A., Margulies, L., Ben-Shlomo, T., Carle, G., Coyne, L.M., Orenberg, J.B., and Scattergood, T.W. 1988. XIX Lunar and Planetary Sci. Conf., 27-28;[5]Morris, R.V., Agresti, D.G., Lauer, Jr., H.C.,Newcomb, J.A., Shelfer, T.D., and Murali, A.V. 1989. J. Geophys. Res., 94, 2760-2778;[6]Evans, D.L. and Adams, J.B. 1979. Proc. Lunar Planet. Sci. Conf. 10th, 1829-1834;[7]Allen, C.C., Gooding, J.L., Jercinovic, M. and Keil, K. 1981. Icarus, 45, 347-369;[8]Singer, R.B.1982.J. Geophys.Res.,87,10159-10168;[9]Roush, T.L., Blaney, D.L., and Singer, R.B. 1990. Remote Geochemical Analysis, K. Pieters and P. Englert, Eds., to be published by ACS in conjunction with LPI;[10]Banin, A. and Margulies, L. 1983. Nature, 305, 523-526;[11]Banin, A, Carle, G.C., Chang, S., Coyne, L.M., Orenberg, J.B., and Scattergood, T.W. 1988. Origins of Life and the Evol. of the Biosph. 18, 239-265;[12]Clark, R.N. and Roush, T.L. 1984. J.Geophys.Res., 89, 6329-6340;[13]Clark, R.N., Swayze, G.A., Singer, R.B., and Pollack, J. 1990. J. Geophys. Res., 95(B9),14463-14480.

A comparison of the diffuse reflectance spectra of different wt % mixtures of palagonite and Fe-montmorillonite (15.8 ±.8 wt % Fe as Fe_2O_3). All spectra are scaled to unity at 1.02 μm.

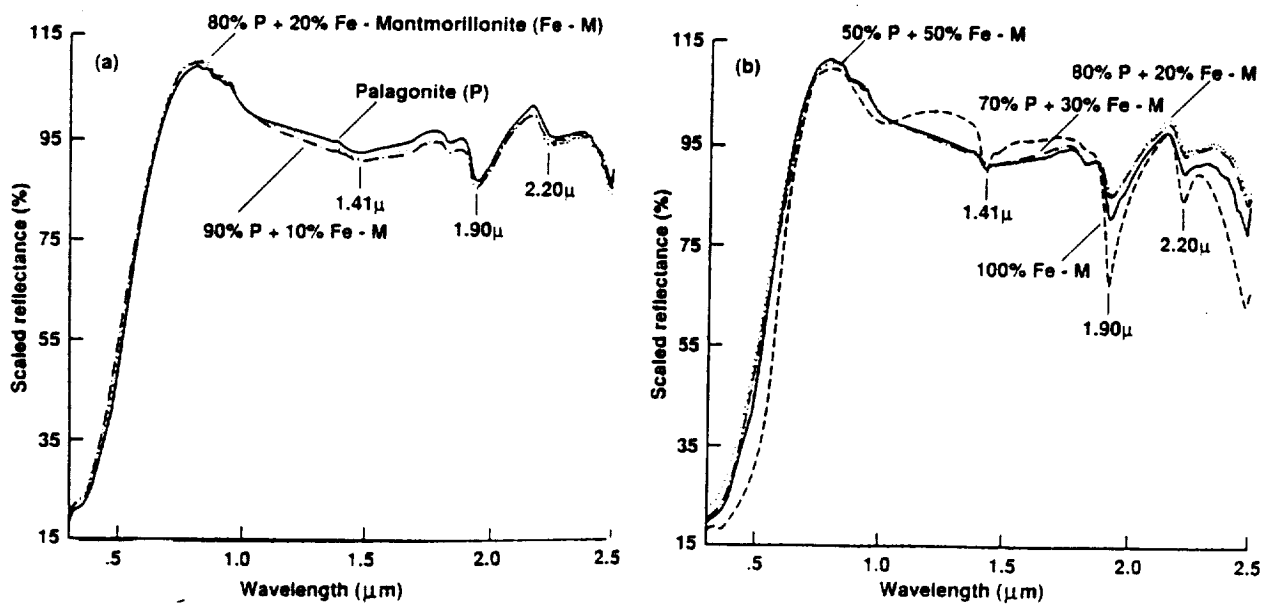

N91-27076

THERMAL AND ALBEDO MAPPING OF THE NORTH AND SOUTH POLAR REGIONS OF MARS; D. A. Paige and K. D. Keegan, Dept. of Earth and Space Sciences, UCLA, Los Angeles, CA 90024.

Here we present the first maps of the thermal properties of the north and south polar region of Mars. The thermal properties of the midlatitude regions from -60° to +60° latitude have been mapped in previous studies[1]. The maps presented here complete the mapping of the entire planet.

The maps for the north polar region were derived from Viking Infrared Thermal Mapper (IRTM) observations obtained between June 10, 1978 to Sept. 30, 1978 (L_s = 98.39 to 121.25, Julian Date = 2443670 to 2443720). This period corresponded to the early summer season in the north, when the north residual water ice cap was exposed, and polar surface temperatures were near their maximum. The maps in the south were derived from observations obtained between Aug. 24, 1977 to Sept. 23, 1977 (L_s = 321.58 to 338.07, Julian Date=2443380 to 2443410). This period corresponded to the late summer season in the south, when the seasonal polar cap had retreated to close to its residual configuration, and the second global dust storm of 1977 had largely subsided. Best fit thermal inertias were determined by comparing the available IRTM 20μ channel brightness within a given region to surface temperatures computed by a diurnal and seasonal thermal model. The model assumed no atmospheric contributions to the surface heat balance. Standard deviations of the model fits were typically less than 3K. Figures 1ab and 2ab show the resulting maps of apparent thermal inertia and average IRTM measured solar channel lambert albedo for the north and south polar regions from the poles to ±60° latitude.

Thus far, the major results of this work can be summarized as follows:

- Surface Water Ice: High albedo, high thermal inertia water ice deposits are widespread within the north residual cap, and in outlying deposits at latitudes as low as +74° . The diurnal thermal inertias derived here are consistent with seasonal thermal inertias derived from measurements of the polar heat balance[2], which implies that these deposits are dense and coherent from the surface to great depths. No surface water ice appears to be present in the southern hemisphere.
- Polar Dune Material: In the north, regions containing low albedo polar dune material can not be distinguished from the surrounding polar planes units solely on the basis of thermal inertia. Regions covered by dunes generally have intermediate thermal inertias, which is consistent with transportation by the martian atmosphere under current climatic conditions. The inertias of the polar dune materials are distinctly lower than the low albedo material that extends northward from the Acidalia region at 45° longitude. Large regions of exposed sand and rock are not present in the south polar region.
- Dust Deposits: The south polar region appears to be the site of a major new low thermal inertia region. The apparent inertias near the south pole are similar to those in the Tharsis and Arabia regions in the northern hemisphere, and are consistend with the presence of a dust layer that extends a depth of at least one diurnal thermal skin depth. The unique location of this deposit may provide clues to the processes responsible for the formation of the northern hemisphere low thermal inertia regions and the layered deposits at both poles. In sharp contrast to the south, there are no extensive regions of contiguous exposed low thermal inertia materials in the north polar region. If the north polar region is presently a major sink for material raised during global dust storms, then this material must be incorporated into the residual water ice deposits.

1. Palluconi, F. D. and H. H. Kieffer, *Icarus* **45**, 415 (1981).
2. Paige, D. A. and A. P. Ingersoll, *Science* **228**, 1160 (1985).

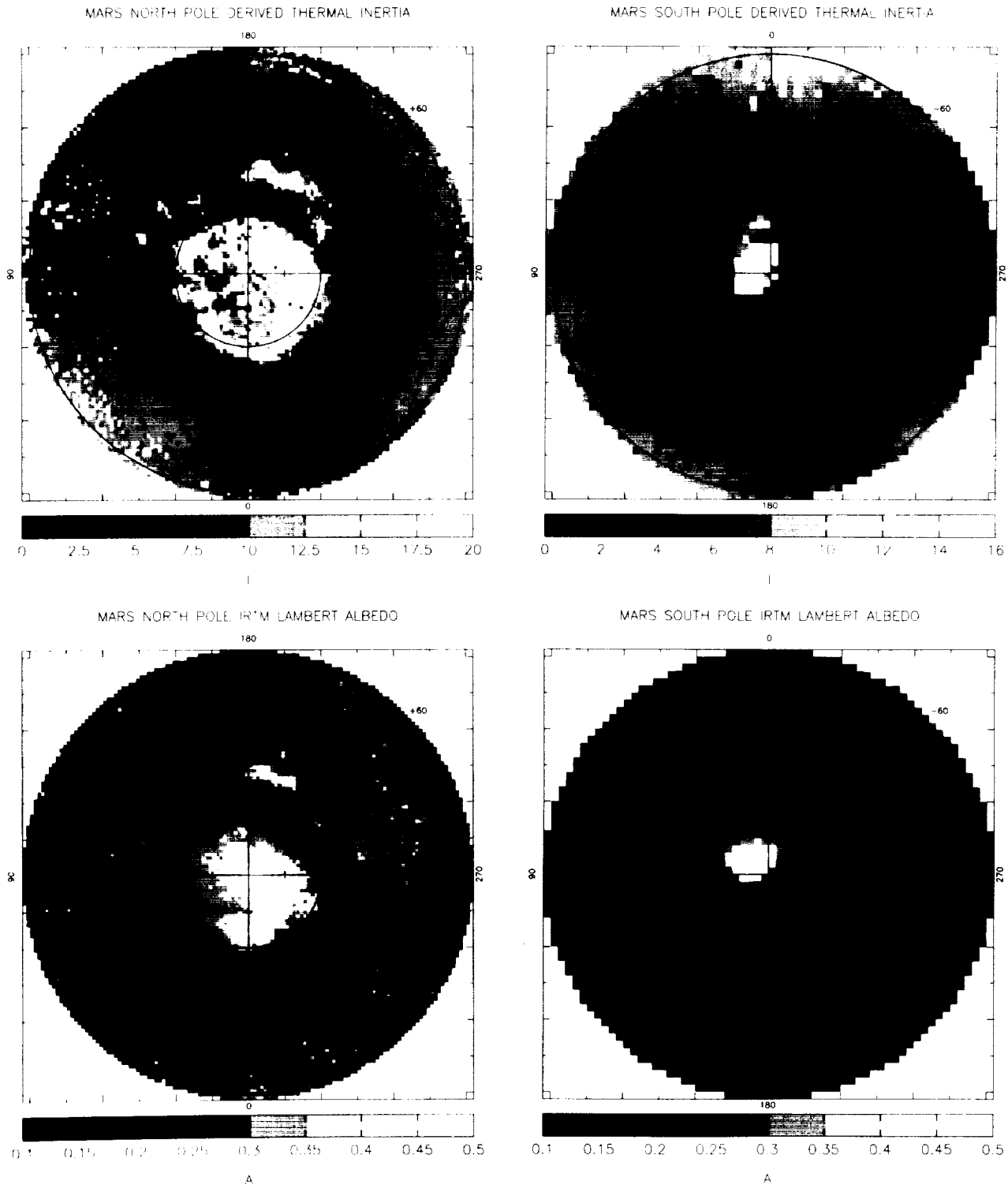

Figures 1-2. Thermal inertia and albedo maps of the north (left) and south (right) polar regions of Mars from Viking IRTM observations. The upper figures show derived thermal inertia in units of $\times 10^{-3}$ cal cm^{-2} $sec^{-1/2}$. The lower figures show measured IRTM Lambert albedo. (data points with values outside the limits of the gray scales below each image were mapped to the highest or lowest gray scale values.)

N91-27077

DERIVATION OF MID-INFRARED (5-25μm) OPTICAL CONSTANTS OF SOME SILICATES AND PALAGONITE

T.L. Roush[1,2], J.B. Pollack[2], and J.B. Orenberg[1], [1]San Francisco State University, [2]NASA Ames Research Center

Recent reports concerning the mid-infrared reflectance properties of silicates [1,2,3] coupled with recent observations of the Earth [4] and other planets [5,6,7,8,9,10] in the mid-infrared and the planned Thermal Emission Spectrometer scheduled as an instrument to be included on the Mars Observer all illustrate the increasing interest in the optical properties of materials in the mid-infrared and their direct application to remote sensing observations of other planetary surfaces. As the laboratory and observational data increase they will ultimately be modeled to aid in the understanding of the composition mineralogy, and distribution of the surface and atmospheric constituents on these bodies.

In order to facilitate such quantitative analyses, knowledge regarding the optical constants (real (n) and imaginary (k) indicies of refraction) of a wide variety of pertinent materials is required. Examples of the application of such quantitative analyses to the interpretation of martian surface and atmospheric constituents, based on the optical constants of minerals, are presented in [8,11,12].

Optical constants can be readily derived from polished surfaces of cohesive materials using standard geological thin sectioning and polishing techniques. The mid-infrared optical constants of only a few specific silicate minerals are available in the literature [12,13,14,15]. Additionally, optical constants have been determined for a number of specific rock types including silicates [14,16] and limestone [17]. Recently optical constants for palagonite, typically a poorly characterized mineralogical assemblage resulting from the alteration of basaltic glass, were presented for a limited wavelength range [18].

This study was initially conceived in order to aid in the interpretation of martian surface and atmospheric aerosol mineralogy. As a result, the minerals included are biased toward samples which represent hydrated and hydroxylated silicates. These include: 1)the Al and Mg end members of the 1:1 layer lattice silicates, kaolinite and serpentine, respectively; 2)an Al-bearing 2:1 layer lattice silicate, pyrophyllite; 3)the Mg and Al smectite clays saponite and montmorillonite, respectively; and 4)a palagonite, typically a poorly characterized alteration product of basaltic glass. Due to their physical particle size clays and other materials, such as palagonite, can not be prepared using typical preparation techniques. Yet in some cases, such as for Mars, these are the materials of perhaps the greatest interest. In order to obtain a suitable sample of these less cohesive materials for the laboratory measurements a KBr pellet die was used and a pellet of the pure sample was prepared. The powders were previously separated by dry sieving and roughly 200 mg of the finest grain size fraction ($\leq$38μm) placed in the KBr die. The die was placed in a hydraulic press and the pressure increased to a maximum of roughly 0.5 to 7 Kbars on the 12mm die, depending upon the sample, and held at that pressure for five minutes. For all clays and the palagonite this produced a pellet with highly reflective surfaces at visible wavelengths.

The reflectivities of all samples were determined by placing them at the focus of a near-normal reflectance attachment located in a Fourier transform spectrometer. The data from each sample was ratioed to the data obtained from a first surface aluminum mirror which was conservatively assumed to have a reflectance of 0.96 at all wavelengths. Data were collected from 4000 to 400 cm^{-1} (2.5-25μm) with a constant spectral resolution of 4 cm^{-1} however, due to an increase in multiple scattering optical constants were derived only in the 2000-400 cm^{-1} (5.0-25μm) region.

To derive the optical constants of a material as a function of wavelength we used the commonly employed technique of dispersion analysis [13,14,15,16,17,19] which describes n and k as the contributions due to a sum of classical oscillators and relates them via Fresnel's equations for non-normal incidence, to the measured near-normal reflectivity. Non-linear least squares techniques was used to minimize the differences between the observed and calculated reflectivities. In our analyses we varied both the total number of oscillators and the high frequency dielectric constant (ε_∞) to most accurately describe the measured reflectances. The final values determined represent averages of several model fits to each data set using the same number of oscillators but varying ε_∞. In all cases we required oscillator central wavelengths to fall within the range of our observations, and the oscillator strengths and widths to be non-negative. The kaolinite and serpentine data were fit with 15 and 10 oscillators, respectively, while the pyrophyllite data required 17 oscillators. The saponite data needed 8 oscillators and the montmorillonite data 15 oscillators. The palagonite data were described by 7 oscillators. For those minerals which contain abundant water, the smectites and palagonite, we were able to include an oscillator for the $\approx$6.25μm H-O-H bending mode.

Overall we found our results were extremely consistent with values previously determined for similar materials [12,15,18] but some discrepancies remain. These discrepancies may be due to differences in analysis techniques, in one study [12] only qualitative assessment of a best fit criteria was used, in another [18] transmission measurements were used along with the assumption that the real index of refraction was constant, and in another study [15] additional measurements at longer wavelengths were included. The discrepancies may also arise from differences in sample composition between the various studies.

References: [1]Salisbury *et al., USGS Open-File Report 87-263,* 1987; [2]Salisbury & Walter, *JGR,* **94,** 9192, 1989; [3]Walter & Salisbury, *JGR,* **94,** 9203, 1989; [4]Bartholomew *et al., J. Remote Sens.,* **10,** 529, 1989; [5]Potter & Morgan, *Proc. 12th Lunar Planet. Sci.,* 703, 1981; [6]Tyler *et al., GRL,* **15,** 808, 1988; [7]Roush *et al., Lunar Planet. Sci. Conf. XX,* 928, 1989; [8]Pollack *et al., JGR,* **95,** 14,595, 1990; [9]Lucey *et al., Bull. Am. Astron. Soc.,* **21,** 970, 1989; [10]Roush *et al., submitted to Lunar Planet. Sci. XXII.* 1991; [11] Aronson & Emslie *JGR,* **80,** 4925, 1975; [12]Toon *et al., Icarus,* **30,** 663, 1977; [13]Spitzer & Kleinman, *Phys. Rev.,* **121,** 1324, 1961; [14]Aronson & Strong, *Appl. Opt.,* **14,** 2914, 1975; [15]Mooney & Knacke, *Icarus,* **64,** 493, 1985; [16]Pollack *et al., Icarus,* **19,** 372, 1973; [17]Querry *et al., Appl. Opt.,* **17,** 353, 1978; [18]Crisp & Bartholomew, *Lunar Planet. Sci. XX,* 201, 1989; [19]Toon *et al., JGR, 81,* 5733, 1976;

N91-27078

ELECTROSTATIC FIELDS IN A DUSTY MARTIAN ENVIRONMENT

D.D. Sentman, Institute of Geophysics and Planetary Physics, University of California, Los Angeles, CA 90024

While there have been several studies suggesting the possibility of electrical activity on Mars, to date there have been no measurements to search for evidence of such activity. In the absence of widespread water clouds and convective storm systems similar to those on the earth and Jupiter, the most likely candidate for the creation of electrostatic charges and fields is triboelectric charging of dust, i.e., the friction between blown dust and the ground, and of dust particles with each other. Terrestrial experience demonstrates that electric fields 5–15 kV-m^{-1} are not uncommon in dust storms and dust devils in desert regions, where the polarity varies according to the chemical composition and grain size. Other familiar examples of dusty environments where this charge-separation mechanism operates, sometimes with lethal effect, are in grain elevators where grain-dust explosions occasionally occur, coal mines, factories where metal dust is prevalent, e.g. ammunition factories, and in volcano plumes. Martian dust storms seem unlikely to produce such extreme conditions as these, but simple laboratory experiments have demonstrated that modest electrostatic fields of roughly 5,000 V-m^{-1} may be produced, along with electrical spark discharges and glow discharges, in a simulation of a dusty, turbulent Martian surface environment. While the Viking landers operated for several years with no apparent deleterious effects from electrostatic charging, this may have been at least partly due to good engineering design utilizing pre-1976 electronic circuitry to minimize the possibility of differential charging among the various system components. However, free roaming rovers, astronauts, and airborne probes (e.g. balloons) may conceivably encounter an environment where electrostatic charging is a frequent occurrence, either by way of induction from a static electric field or friction with the dusty surface and atmosphere. This raises the possibility of spark discharges or current surges when subsequent contact is made with other pieces of electrical equipment, and the possibility of damage to modern microelectronic circuitry. Measurements of electrostatic fields on the surface of Mars could therefore be valuable for assessing this danger. Electric field measurements could also be useful for detecting natural discharges that originate in dust storms. This detection could be performed at distances ranging from 10s of km in the case of J-change-like discharge signatures, to planetary distances if there exists a global electrical circuit or Schumann resonance spectrum. Measurement of the horizontal electric (telluric) fields may also yield information concerning the dayside ionospheric convection electric field produced by the interaction of the solar wind with the Martian atmosphere.

N91-27079

IMPACT OF MARS SAND ON DUST ON THE DESIGN OF SPACE SUITS AND LIFE SUPPORT EQUIPMENT - A TECHNOLOGY ASSESSMENT

Charles H. Simonds, Lockheed Life Support Development Laboratory,
Mail Code A-23, 1150 Gemini Ave., Houston, Texas 77058-2742

Space suits and life support equipment will come in intimate contact with Martian soil as aerosols, wind blown particles and material thrown up by men and equipment on the Martian surface. For purposes of this discussion the soil is assumed to consist of a mixture of cominuted feldspar, pyroxene, olivine, quartz, titanomagnetite and other anhydrous and hydrous iron bearing oxides, clay minerals, scapolite and water soluble chlorides and sulfates. The soil may have photoactivated surfaces that acts as a strong oxidizer with behavior similar to hydrogen peroxide.

Bearings and seals - The rotary joints used on state of the art Space Suit Assemblies such as the Ames AX-5 or the JSC Mark III are ball bearing joints integrated with one or more pressure-assisted lip seals. Both lubricated and dry bearing have been developed and either approach must be considered in any potential Mars walking suit. These bearings and seals will have to be protected with a dust restraining seal on both the inside and outside of the suit. The inside seal is to prevent grit introduced during servicing from getting into the bearings. Designing these dust inhibiting seals will be a design challenge because the total mass of the space suit must be strictly controlled to remain within a human's carrying capacity.

Linear actuators, ball screws - Various kinds of linear actuators and ball screws are likely on Mars equipment. Like the space suit bearings they must be designed so that any adhering dust is kept away from any close tolerance meshing surfaces. The magnetic attraction of the soil will also be considered in designing any device to wipe the soil off the meshing surfaces. Standard terrestrial aircraft practice could provide a point of departure for such designs or the machine-tool practice of covering linear actuators with elastomeric bellows could be followed.

Gas inlets to compressors or other devices - A wide variety of indigenous resource utilization schemes using the Mars atmosphere have been proposed. A common feature of this equipment is a mechanical or chemical compressor drawing in large volumes of the Mars atmosphere. Certainly gas inlets will have to have dust filters just as they would on Earth. Designing such filters will not be a major challenge.

Heat exchangers rejecting heat to the Martian atmosphere - The fine passages of compact heat exchangers must be protected from a build up of dust and grit. The design of the filters for this purpose will be more of a challenge than for the compressor inlets because the heat exchanger flow rates will be orders or magnitude greater. The filters will have to be very efficient to minimize pressure drop and unacceptably large power demands. Nonetheless the problem is a relatively straight forward one.

Pressure seals - Space suits and other equipment will contain numerous pressure seals which are repeatedly made up and disassembled on the Martian surface during the course of a mission. These seals inevitably will become contaminated with some soil. Conventional elastomeric seals such as O-rings are quite tolerant of such contamination unlike knife edge or other metal to metal seals. The major impact of the dust will be operational rather than on design. Even the most dust tolerant sealing system will demand that the seals and connections be wiped off each time they are made up.

Thermal protection garments - Thermal protection on the Martian surface will be quite different from the Moon during Apollo, because the Mars environment is cold and the atmosphere has a significant gas thermal conductivity. However, during daylight EVA the convective and radiation losses from a space suit will be significantly less than the the metabolic and electric heat generated in the EMU. The design challenge will thus be to keep the astronaut's arms, legs, hands, and feet

warm while still having a net heat loss. Because the crew's extremities must be kept warm they will be heavily insulated. Unlike during Apollo lunar surface EVA, the increase in absorbance of visible and thermal i-r radiation due to an adhering soil coating will not adversely affect performance. Insulation will have to be similar to that used on earth with numerous small trapped gas spaces. Despite the low pressure, the thermal conductivity of the Mars atmosphere is large enough that Multi-Layer Insulation which prevents radiative heat transfer will not be effective. However, insulation approaches used in the Arctic should be effective.

Optical surfaces, radiators, and helmets - Optical surfaces will become contaminated with dust, which will have to be carefully removed to prevent scratching. Should radiators be selected as part of the heat rejection scheme, some provisions will have to be made to remove adhering dust. The dust will have to removed carefully, because current state-of-the-art low-solar-absorbance high-thermal i-r emissivity coatings are a multi-layer laminate of coated films which are not scratch resistant.

Materials constraints on pressurized volume coming in contact with the soil - The Mars astronauts will inevitably track soil into the pressurized volume exposing the soil to warm moist air. Some constituents of the soil are probably hygroscopic and any soil which comes in contact with moist air at room temperature will yield a salt solution, probably with an acidic pH. Thus any equipment which comes in contact with soil-contaminated moisture must be corrosion resistant. However fairly straight forward material control can emphasize use of corrosion resistant alloys possibly at the sacrifice of some strength, e.g. selection of 6061 aluminum alloy in preferences to the stronger but less corrosion resistant 7075. If the soil has a high level of chemical activity, as suggested by the biological experiments on Viking, it may attack some organic materials once it gets inside the pressurized volume. The impact of that chemical activity is the one aspect of the soil which could have the most significant impact on space suit and life support equipment design. However, if the the activity can be modeled as that of a peroxide or superoxide. Thus a series of tests to determine materials degradation and offgassing upon exposure to solid or liquid peroxides should define the magnitude of any physical degradation or generation of toxic vapors. Even if traces amounts of noxious gases should be generated, their significance may be quite small. the concentrations should be those levels can be evaluated in terms of the Spacecraft Maximum Allowable Concentration (SMAC) levels, and the performance of traces contaminant removal systems used on the Shuttle Orbiter or proposed for Space Station Freedom.

Summary - The existing data about the Mars soil suggests that the dust and sand will require designs analogous to those uses on equipment exposed to salt air and blowing sand and dust. The major design challenges are in developing high performance radiators which can be cleaned after each EVA without degradation, designing seals that are readily cleaned and possibly in selecting materials which will not be degraded by any strong oxidants in the soil.

The magnitude of the dust filtration challenge needs careful evaluation in terms of the trade off between fine-particle dust filters with low pressure drop that are either physically large and heavy, like filter "baghouses,", require frequent replacement of filter elements, of low volume high pressure drop thus power consumption approaches, or washable filters. In the latter, filter elements are be cleaned with water, as could the outsides of the space suits (properly designed, of course) in the airlock.

N91-27080

SAND AND DUST ISSUES FOR THE MESUR MISSION

P. F. Wercinski and G. S. Hubbard, NASA Ames Research Center

The presence of particles in the Martian atmosphere increases the rate of erosion of the heat shield during the entry phase of the MESUR mission. Preliminary analysis has shown that under certain conditions particles will penetrate the bow shock of the entry vehicle, impact and erode the heat shield, above the anticipated rate from the ablation process. Knowledge of the distribution, sizes, and composition of particles suspended in the atmosphere will permit the estimation of the heat shield recession both for a nominal Mars atmosphere and in dust storm conditions. Some key interests concerning sand and dust in the atmosphere can be summarized in the following questions.

1) What is the variation of atmospheric dust distribution for nominal atmospheric conditions as well as in dust storm conditions as a function of altitude, latitude & longitude, and season?
2) What level of predictive capability exists i) at present, and ii) with MO, to forecast the onset of a dust storm?
3) What is the ratio of dust to gas in the atmosphere?
4) What is the distribution of particle sizes?
5) What is the best estimate of the compositional nature of particles in the atmosphere, i.e. what percentage of the particles are silicate and what fraction is ice? This is important in estimating the fraction of particles that will impact the heat shield surface. Knowledge of the composition of the dust particles is also needed to determine the extent of their sublimation in the shock layer.

On the surface of Mars, sand and dust can effect of the operations and design of the science instruments (i.e. imaging) and lander subsystems (i.e. solar arrays). Distribution and deposition of sand and dust on the planet's surface will dictate the feasibility of using solar arrays as a power source for the lander. Furthermore, the potential abrasive nature of blowing particles must be understood in order to properly select suitable materials for lander structure and any components exposed to the environment. The selection of lander material may also be dictated by corrosive and chemically active properties of particles at a potential landing site. Some key interests concerning sand and dust on the surface can be summarized in the following questions.

1) What factors determine the distribution and deposition of sand and dust on the surface?
- winds
- local geography (for example, does landing on the leeward side of a mountain, hill, or just a big rock, greatly effect the distribution of dust either by winds or the presence of sand and dust sources)
- local geology (lava flows, craters, etc.)
- regions of active sand dunes
- other meteorological factors

2) What is the current state of knowledge concerning deposition of sand and dust on surface landers?
- electrostatic properties
- Viking design requirements
- deposition on solar arrays
- abrasion effects of blowing sand on s/c materials (design goal for up 8 earth-years on surface)

3) How could the Mars wind tunnel at Ames be best used during FY91 for determining answers to any of the above mentioned questions?

N91-27081

MARTIAN DUST THRESHOLD MEASUREMENTS - SIMULATIONS UNDER HEATED SURFACE CONDITIONS

Bruce R. White, Department of Mechanical Engineering, University of California, Davis, CA 95616 and Ronald Greeley and Rodman N. Leach, Geology Department, Arizona State University, Tempe, AZ 85201

Diurnal changes in solar radiation on Mars set up a cycle of cooling and heating of the planetary boundary layer, this effect strongly influences the wind field. The stratification of the air layer is stable in early morning since the ground is cooler than the air above it. When the ground is heated and becomes warmer than the air its heat is transferred (by molecular conduction action - no flow at the ground) to the air above it. The heated parcels of air near the surface will, in effect, increase the near surface wind speed or increase the aeolian surface stress the wind has upon the surface when compared to an unheated or cooled surface.

This means that for the same wind speed at a fixed height above the surface, ground-level shear stress will be greater for the heated surface (unstable case) than an unheated surface. Thus, it is possible to obtain saltation threshold conditions at lower mean wind speeds when the surface is heated. Even though the mean wind speed is less when the surface is heated, the surface shear stress required to initiate particle movement remains the same in both cases.

To investigate this phenomenon, low-density surface dust aeolian threshold measurements have been made in the MARSWIT wind tunnel located at NASA Ames Research Center, Moffett Field, California. The MARSWIT is an open circuit wind tunnel that is operated within a large pressure chamber (4000 m^3) that allows a range in operating pressure from a few millibar to one atmosphere of pressure (Greeley et al., 1977). The current experiments were carried out with both heated and unheated surface temperature conditions. The heated surface condition represents or models diurnal surface heating by radiation from the sun. The unheated surface represents a neutrally stable condition. The heating of the floor primarily affects the vertical turbulent structure of the boundary layer. The exact level of heating is unknown under Mars surface conditions; however, it is expected to produce a maximum temperature difference of 25 K between the surface and the atmosphere above it. (Hess et al. 1977; Ryan and Henry, 1979).

Limited vertical temperature profiles also were measured under several heating conditions which enabled a determination of friction speed, u_* as a function of freestream speed at a specified heating condition. Additionally, the surface material temperature was measured with a thermocouple from which the value of bulk Richardson number was determined.

On Mars, from the Viking Landers, there are no direct data available as to the mean wind speed and surface temperature when the initial dust movement occurred. However, Arvidson, et al. (1983) estimate that winds of 25 to 30 m/s would be needed to initiate particle motion of optimum sized surface material (i.e., about 100 microns in mean diameter). Presumably this would occur at Mars noon when the temperature difference between the surface and Lander was a maximum. For the Lander case this corresponds to a bulk Richardson number of about -0.02 at threshold.

The experiments were carried out for two different sized particles, one having a mean diameter of about 105 microns while the other sample material had a mean diameter of about 11 microns. Threshold measurements were made under two surface temperature conditions: one where the surface was not heated (i.e., uniform temperature throughout the boundary layer profile) and the other where the surface was heated. The amount of surface heating was varied for each experiment and approximately represents a value of bulk Richardson number from zero to -0.02 which is believed to be in the range that exist on the surface of Mars near the Viking Lander sites.

The first series of tests examined threshold values of the 100 micron sand material. At 13 mb surface pressure the unheated surface had a threshold friction speed of 2.93 m/s (and approximately corresponded to a velocity of 41.4 m/s at a height of 1 meter) while the heated surface, equivalent bulk Richardson number of -0.02, yielded a threshold friction speed of 2.67 m/s (and approximately corresponded to a velocity of 38.0 m/s at a height of 1 meter). This change represents an 8.8% decrease in threshold conditions for the heated case. The values of velocities are well within the threshold range as observed by Arvidson et al., 1983. Figure 1

presents this data. As the surface was heated the threshold speed decreased. At a value of bulk Richardson number equal to - 0.02 the threshold friction speed and threshold wind speed appeared to level-off to a constant value.

This trend also was observed in the MARSWIT experiments involving the 11 micron sized-silt material. Although we were not able to directly measure extensive numerical values to support this trend, it was readily observed in the tunnel testing. Note, it is extremely difficult to maintain constant ambient chamber pressure while continuously increasing the wind flow through the tunnel. Figure 2 does, however, present the two data points that have been measured to date. The threshold friction speed at 6.7 mb pressure of the 11 micron dust material was found to be 9.4 m/s with the unheated surface. When the surface was heated to a value of bulk Richardson number equal to -0.01, the friction threshold speed was reduced by 18% to a value of 7.7 m/s. Unfortunately, this is the only ambient chamber pressure (6.7 mb) that the MARSWIT was able to achieve threshold conditions.

The data results suggest that as the surface is heated the threshold wind speed will decrease. The amount reduction in threshold wind speed appears to be a function of bulk Richardson number as well as the mean size of the test material. The smaller sized materials will tend to experience more of a reduction in threshold wind speed. It is anticipated that for larger size particles there will be negligible difference between heated and unheated surfaces (larger than 1 mm in diameter) in values of threshold wind speed.

REFERENCES

Arvidson, R.E., E.A. Guinness, H.J. Moore, J. Tillman, and S.D. Wall, Three Mars Years: Viking Lander I Imaging Observations, Science, Volume 222, Number 4623, pp. 463-468.

Greeley, R., B.R. White, J.B. Pollack, J.D. Iversen, and R.N. Leach, Dust Storms of Mars: Considerations and Simulations, NASA Tech. Memo., TM 78423, 1977.

Hess, S.L., R.M. Henry, C.B. Leovy, J.A. Ryan, and J.E. Tillman, Meterological Results From the Surface of Mars: Viking 1 and 2, Journal of Geophysical Research, Volume 82, No. 28, pp. 4559-4574.

Ryan, J.A. and R.M. Henry, Mars Atmospheric Phenomena During Major Dust Storms, as Measured at Surface, Journal of Geophysical Research, Volume 84, No. 86, pp. 2821-2829.

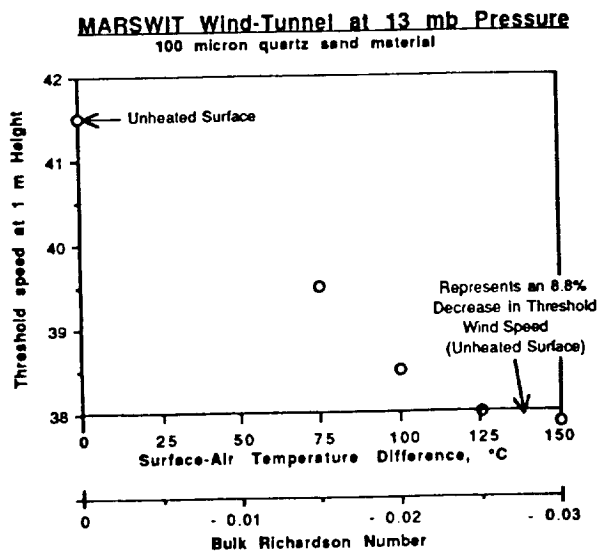

Figure 1. Threshold wind speeds and Bulk Richardson Numbers for 100 micron diameter Quartz sand.

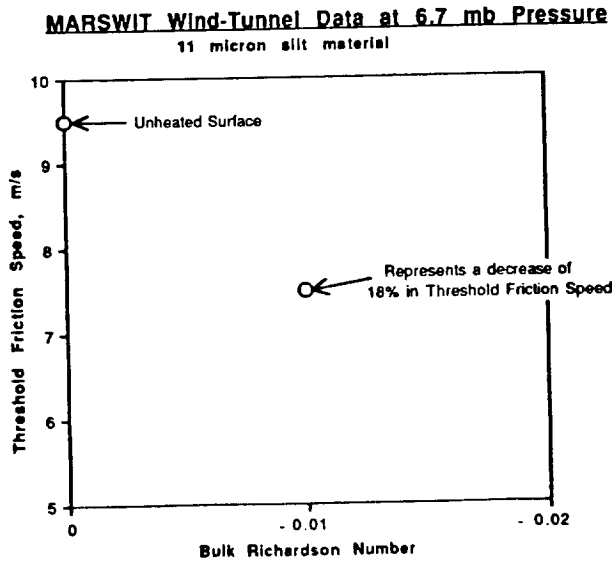

Figure 2. Threshold Friction Speeds for 10 micron diameter silt.

N91-27082

DUST IN THE MARS ATMOSPHERE

R. W. Zurek and R. M. Haberle, JPL/Caltech and NASA Ames Research Center

The amount of dust suspended in the Martian atmosphere is highly variable with location and with time. The opacity of the sky is best known at the two Viking Lander sites, where the visual, vertical-column optical depth never fell below a value of a few tenths during the 1 and 1/4 Mars years of observations and yet exceeded 2-3 during two great dust storms in 1977. Elsewhere on the planet, optical depths have been estimated from orbiter visible imaging of surface contrasts and from mapping of infrared emission from the surface and the overlying (dusty) atmosphere. In many cases these opacities (and thus dust amounts) may be uncertain by as much as a factor of two.

Spacecraft and Earth-based observations have revealed local, regional and planet-encircling dust storms. Local storms occur most frequently, are relatively short-lived, and may occur in any season. The larger dust storms are relatively infrequent, are longer-lived, and tend to originate during southern spring and summer. By no means do they occur in every Mars year, and when they do occur, there are vast differences in their longevity and areal coverage. The greatest dust storm observed on Mars began in 1971 before the arrival of Mariner 9, obscured nearly all of the planet's surface for several months, and raised dust up above 50 km in altitude.

Such storms have been observed to alter substantially the global fields of atmospheric temperature, density and wind. General circulation modeling indicates that the rapid development and the variability of these storms are due to a radiative-dynamic feedback in which suspended dust absorbs solar radiation, heats the atmosphere and thereby alters pressure gradients. This,in turn, modifies the winds raising dust into the atmosphere and redistributing it across the planet.

Viking Lander observations of twilight indicate that the background dust haze is more or less uniformly mixed with altitude in the lower atmosphere. Observations from spacecraft indicate that there may be some seasonal variation to the height of these dust hazes, which sometimes extend above 30 km. (Ice haze layers may occur as high as 80 km.) During local dust storms, most of the suspended dust comprising the storm is confined below 20 km. During larger dust storms, however, micron-sized dust particles may be mixed to higher altitudes.

The existing observations do not constrain the composition or the size distribution of the suspended dust particles very well. Remote sensing observations depend principally upon the product of the number of particles, the geometric cross-sections (and so particle size and shape), and the extinction efficiency of the particles (and so the particle composition), as integrated over the particle size distribution and along the line of sight. While the observed variation of dust opacity with wavelength constrains these quantities, it does not often permit the unique determination of the individual properties of the suspended dust.

A size distribution having a cross-section weighted mean particle radius of 2.5 μm was deduced from a synthesis of the IR thermal emission spectra observed in the southern hemisphere by Mariner 9 during the 1971 global dust storm. Although the IR thermal emission is relatively insensitive to the sub-micron sized particles which tend to dominate visible opacity, this same size distribution was consistent with modeling of the sky brightness variation near the sun, as seen through the background haze above the Viking Lander sites, in the northern hemisphere.

However, the ratio of infrared opacity inferred from the Viking Orbiter data to the visible opacity derived by direct imaging of the sun from the Viking Landers differs by a factor of two from that predicted using the canonical (Mariner 9) size distribution. Model fits using smaller particles or particle aggregates have been proposed to resolve this discrepancy, but remain to be tested fully. Furthermore, model simulations of the evolution of the size distribution of dust particles suspended during a great dust storm indicate that considerable spatial and temporal variability in that size distribution should occur.

Observed thermal IR spectra indicate that dust suspended in the atmosphere is a mixture dominated by igneous silicates containing mainly SiO_2 (> 60%), or by weathering products such as clay minerals, perhaps with some basalt also present. At visible wavelengths, the optical depth of the suspended dust tends to be dominated by trace materials; analysis of the Viking Lander images of sky brightness were consistent spectrally with particles having a trace ($\approx$1% by volume) of magnetite.

Future missions to Mars can greatly augment the global, seasonal and interannual observational coverage of dust suspended in the Martian atmosphere. Starting near the end of 1993, instruments onboard the Mar Observer spacecraft, orbiting Mars in a low, circular and nearly polar orbit, will map the distribution of atmospheric dust, including its vertical distribution, globally each day for one and perhaps two Mars years. A combination of IR thermal emission and broadband visual observations, taken in both limb and on-planet viewing modes, will be used. Constraints on particle size and bulk composition similar to those derived from the Mariner 9 and Viking data will be provided, but with systematic global coverage and higher spatial resolution. The MARS 94 mission will also provide visual and thermal emission data and, in addition, is likely to acquire solar and stellar occultation data which can be used to further constrain dust particle properties. Present plans also include direct collection and optical characterization of suspended dust using the other platforms (i.e., balloons, penetrators, mini-rovers) to be deployed as part of the MARS 94 mission.

Monitoring of the sky brightness by surface instruments deployed as part of the proposed MESUR mission could provide multi-year time series of precise overhead opacity measurements and of general constraints on the microphysical properties of suspended dust particles at several locations distributed over the globe, including southern hemisphere, polar, and high altitude sites, all of which are likely to differ from the two low-lying Viking Lander sites. Sampling of suspended dust during the entry of the MESUR landers could also provide more definitive characterizations of the dust particle properties.

Acknowledgement. This research was performed at the Jet Propulsion Laboratory, California Institute of Technology and at the NASA Ames Research Center and was supported in part by NASA's Planetary Atmospheres Program.

NASA
National Aeronautics and Space Administration

Report Documentation Page

1. Report No.	2. Government Accession No.	3. Recipient's Catalog No.
NASA CP-10074		

4. Title and Subtitle	5. Report Date
Sand and Dust on Mars	May 1991
	6. Performing Organization Code

7. Editor(s)	8. Performing Organization Report No.
Ronald Greeley (Department of Geology, Arizona State University, Tempe, Arizona 85287-1404) and Robert Haberle	A-91130
	10. Work Unit No. 151-01-60-03
9. Performing Organization Name and Address	11. Contract or Grant No.
Ames Research Center Moffett Field, CA 94035-1000	NCC2-346
	13. Type of Report and Period Covered
12. Sponsoring Agency Name and Address	Conference Publication
National Aeronautics and Space Administration Washington, DC 20546-0001	14. Sponsoring Agency Code

15. Supplementary Notes

Point of Contact: Robert Haberle, Ames Research Center, MS 245-3, Moffett Field, CA 94035-1000
(415) 604-5491 or FTS 464-5491

16. Abstract

Mars is a planet of high scientific interest. Various studies are currently being made that involve vehicles that have landed on Mars. Because Mars is known to experience frequent wind storms, mission planners and engineers require knowledge of the physical and chemical properties of martian windblown sand and dust, and the processes involved in the origin and evolution of sand and dust storms. Consequently, a workshop was organized for February 4-5, 1991, at Arizona State University to provide a forum for discussion involving mission planners, and members of the scientific community who are interested in sand and dust on Mars. This document contains the contributions from the participants at the workshop.

17. Key Words (Suggested by Author(s))	18. Distribution Statement
Mars, Sand, Dust, Aeolian, Electrostatics, Sand storms, Dust storms, Wind erosion, Martian mineralogy	Unclassified-Unlimited Subject Category – 91

19. Security Classif. (of this report)	20. Security Classif. (of this page)	21. No. of Pages	22. Price
Unclassified	Unclassified	66	A04

NASA FORM 1626 OCT 86

For sale by the National Technical Information Service, Springfield, Virginia 22161